6-26-2015

Second law analysis and the application of the efficient power criterion to a four-temperature-level absorption chiller

Dionicio Rios

Dionicio F. Rios

Candidate

Mechanical Engineering

Department

This thesis is approved, and it is acceptable in quality and form for publication: Approved by the Thesis Committee:

Dr. Arsalan Razani, Chairperson

Dr. C. Randall Truman

Dr. Svetlana Poroseva

SECOND LAW ANALYSIS AND THE APPLICATION OF THE EFFICIENT POWER CRITERION TO A FOUR-TEMPERATURE-LEVEL ABSORPTION CHILLER

by

DIONICIO F. RIOS

BACHELOR OF SCIENCE IN

MECHANICAL ENGINEERING

THE UNIVERSITY OF NEW MEXICO, 2012

THESIS

Submitted in Partial Fulfillment of the
Requirements for the Degree of

MASTER OF SCIENCE

MECHANICAL ENGINEERING

The University of New Mexico
Albuquerque, New Mexico

MAY 2015

SECOND LAW ANALYSIS AND APPLICATION

OF THE EFFICIENT POWER CRITERION TO A

FOUR-TEMPERATURE-LEVEL

ABSORPTION CHILLER

By

Dionicio F. Rios

B.S., Mechanical Engineering, The University of New Mexico, 2012.

M.S., Mechanical Engineering, The University of New Mexico, 2015

ABSTRACT

Absorption chillers are a good option for air-conditioning applications and can be operated by low grade energy which makes them environmentally friendly. Common absorption chillers have four main internal components (generator, evaporator, condenser and absorber) and operate between four temperature levels (which are assumed to be of infinite heat capacity in most studies). Heat transfer interactions that occur between the heat reservoirs and the internal components are of high importance to determine the efficiency and cooling capacity of absorption chillers. The purpose of this study is to quantify the performance of an absorption chiller that interacts with finite heat capacity reservoirs. To accomplish this, the effectiveness-NTU method is applied to an infinite heat capacity model in order to derive a finite heat capacity model. Then, a second law analysis along with a thermo-ecological criterion is applied to determine the best compromise between efficiency and cooling load. System's input parameter variations are an important tool, while determining the efficiency-cooling capacity compromise. With the results found in this study, insight into future research regarding this type of systems will be gained.

Table of Contents

List of Figures

List of Tables

Nomenclature

$\dot{E}_{des}$	Rate of exergy destruction of the system
$\dot{Q}_A$	Rate of heat transfer between heat reservoir and absorber
$\dot{Q}_C$	Rate of heat transfer between heat reservoir and condenser
$\dot{Q}_E$	Rate of heat transfer between heat reservoir and evaporator
$\dot{Q}_G$	Rate of heat transfer between heat reservoir and generator
$\dot{Q}_L$	Rate of heat leakage
$\dot{S}_{gen}$	Entropy generation
$\dot{W}_\eta$	Efficient power criterion
$A_{1,G}$	Surface area of heat exchanger interacting with the generator
$A_{2,E}$	Surface area of heat exchanger interacting with the evaporator
$A_{3,C}$	Surface area of heat exchanger interacting with the condenser
$A_{4,A}$	Surface area of heat exchanger interacting with the absorber
C_h	Heat capacity rate, hot
C_c	Heat capacity rate, cold
C_{max}	Heat capacity rate, max
C_{min}	Heat capacity rate, min
$\dot{E}$	Ecological criterion (Curzon & Ahlborn. Er al 1975)
E_{bal}	Energy balance
K_L	Heat leakage coefficient
L_{HX}	Length of heat exchanger
$Q_{A,abs,4}$	Heat released from the absorber
$Q_{C,cond,3}$	Heat released from the condenser
$Q_{E,evap,2}$	Heat input from cooling load to evaporator
$Q_{G,gen,1}$	Heat supplied from heat source to generator
R_{COP}	Cooling load of system

R_{max}	Maximum cooling load of system
R_{ε}	Cooling load of system
T_0	Temperature of heat reservoir interacting with condenser
T_1	Working fluid temperature in the generator
T_2	Working fluid temperature in the evaporator
T_3	Working fluid temperature in the condenser
T_4	Working fluid temperature in the absorber
$T_{h,i}$	Temperature hot, in
$T_{h,o}$	Temperature hot, out
T_A	Temperature of heat reservoir interacting with absorber
T_{A1}	Inlet temperature of heat reservoir interacting with the absorber
T_C	Temperature of heat reservoir interacting with condenser
T_{C1}	Inlet temperature of heat reservoir interacting with the condenser
T_{CA}	Temperature ratio for COP_{car}
T_E	Temperature of heat reservoir interacting with evaporator
T_{E1}	Inlet temperature of heat reservoir interacting with the evaporator
T_G	Temperature of heat reservoir interacting with generator
T_{G1}	Inlet temperature of heat reservoir interacting with the generator
T_H	Temperature of heat reservoir interacting with generator
T_L	Temperature of heat reservoir interacting with evaporator (cold reservoir)
T_M	Temperature of heat reservoir interacting with absorber
$T_{c,i}$	Temperature cold, in
$T_{c,o}$	Temperature cold, out
$T_{o,env}$	Ambient temperature
$U_{1,G}$	Overall heat transfer coefficient of heat exchanger interacting with the generator

$U_{2,E}$	Overall heat transfer coefficient of heat exchanger interacting with the evaporator
$U_{3,C}$	Overall heat transfer coefficient of heat exchanger interacting with the condenser
$U_{4,A}$	Overall heat transfer coefficient of heat exchanger interacting with the absorber
$\dot{W}$	Power input/output
$\dot{m}$	Mass flow rate
q_{max}	Maximum possible heat transfer rate
a	Heat reject ratio between absorber and condenser
COP	Coefficient of performance
e, ψ	Physical exergy
E_COP	Exergetic efficiency
E_max	Maximum ecological function
ECOP	Ecological coefficient of performance (Ust, Y., Sahin, B. et al 2005)
ECOP_max	Maximum ecological coefficient of performance
ECOP1	Efficient power criterion for absorption chiller
ECOP2	Thermo-ecological criterion for absorption chiller
EES	Engineering Equation Solver
eff	Heat exchanger effectiveness
eff-NTU	Effectiveness-NTU method
FTT	Finite time thermodynamic method
h	Enthalpy
I	Internal irreversibility factor
s	entropy
COP_{car}	Coefficient of performance for reversible Carnot cycle

Subscripts

A	Absorber
A,i	Absorber, in
A,o	Absorber, out
C	Condenser
C,i	Condenser, in
C,o	Condenser, out
E	Evaporator
e	exit/outlet
E,i	Evaporator, in
E,o	Evaporator, out
G	Generator
G,i	Generator, in
G,o	Generator, out
i	inlet
j	Relation between heat reservoir and internal component
o	Environmental condition

Greek symbols

$\dot{\sigma}_{gen}$	Entropy generation/rate of entropy production
ε_{max}	Maximum coefficient of performance
ε	Coefficient of performance
η	Efficiency
Ξ	heat rejection ratio between the absorber and the whole system
Σ	Summation

1.0 Introduction

Existing cooling technologies employ either electricity or heat energy in order to perform their intended operations. An example of these cooling technologies is an absorption chiller, which is the main focus of this paper. An absorption chiller is an example of heat-driven technology employed to transfer heat from a low temperature to a high temperature (cooling/refrigeration cycle). There are different types of absorption chillers ranging from direct-fired, indirect-fired to single, double or triple-effect. The type of absorption chiller to be analyzed in this paper is a single-effect, indirect-fired model coupled to external heat reservoirs. A single-effect absorption refrigerator/chiller is the simplest form of absorption refrigeration cycles. It consists primarily of a generator, an evaporator, a condenser and an absorber. It normally transfers heat between three temperature levels but very often between four temperature levels, as it will be discussed in later sections (Chen et al., 1999; Kaushik S. et al 1983; Abrahamsson k. et al 1993). Many single-effect absorption chillers that use low pressure steam or hot water as the heat source have been installed in commercial buildings to produce chilled water for air conditioning applications (Farchad, P. Z. et al 2011; Garland, R. W. et al 1996; Tang, T. et al 1998; Herold, K. E. et al 1996). Absorption chillers are also a viable replacement to their counter parts, vapor compression chillers, as these are driven by low grade energy (steam, waste heat) as opposed to high grade energy (electricity). Many industrial processes reject a considerable amount of waste heat to the surroundings at a temperature high enough above ambient temperature to make waste heat recovery economically attractive. Because of the nature of the heat source that drives the indirect-fired absorption chillers, these systems have a large potential for reducing the pollution introduced to the environment (Chen, L. et al 2006; Ziegler, F. et al 2002; Chen, J. et al 1999).

The simplest absorption chiller cycle is presented in figure 1, where it is shown that a mechanical compressor, driven by an electric motor (high grade energy), provides the work input that drives the heat transfer from the low temperature to the high temperature

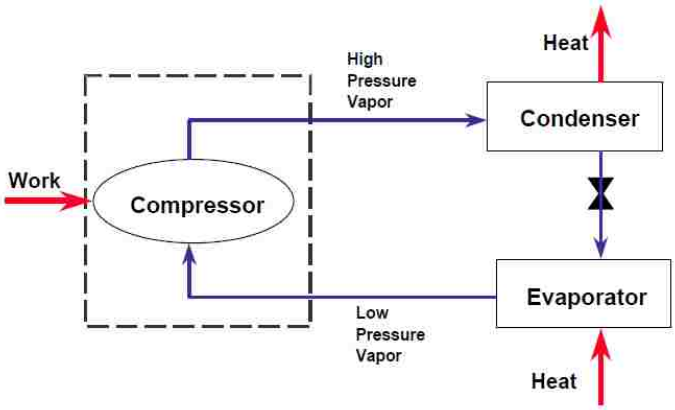

*figure 1: Simple absorption cycle powered by an electrically driven compressor. (*Tang , T., Villareal, L., Green, J. et al 1998)

In the absorption chiller cycle, shown in figure 1, the evaporator allows the refrigerant to evaporate and to be absorbed by the absorbent, a process that extracts heat from the building. The combined fluid then goes to the generator, which is heated by the heat source, driving the refrigerant back out of the absorbent. The refrigerant then goes to the condenser to be cooled down to a liquid, while the absorbent is pumped back to the absorber. The cooled refrigerant is released through an expansion valve into the evaporator, and the cycle repeats (Tang , T. et al 1998).

Plenty of research has been conducted regarding the performance optimization of single-effect, indirect-fired, four-temperature-level absorption chillers. The research shows that the finite time thermodynamic (FTT) method is an important tool while determining fundamental optimal relationships between the maximum coefficient of performance (COP)

and the cooling load for single-effect absorption chillers. This study seeks to improve the performance optimization process for an indirect-fired, single-effect absorption chiller system coupled to external heat reservoirs. This will be done by analyzing the interactions between the heat reservoirs and the individual components of the system (generator, evaporator, condenser and absorber) in order to identify and determine the best compromise between the efficiency (COP) and cooling load of the whole system. The irreversibility distribution of major components of the system will be determined. The total efficiency and the cooling load capacity will be calculated by applying the first and second law of thermodynamics to the system and the irreversibility distribution of major components will be determined. Then, these will be compared and analyzed in order to determine the optimal operational parameters the system must meet to achieve the highest possible efficiency (COP) at the highest possible cooling load capacity. Furthermore, an infinite heat capacity analysis and a finite heat capacity analysis combined with the effectiveness – NTU ($eff - NTU$) method will be applied to the model to generate a more realistic system model and obtain more significant results in the process (sec. 3.5). Finally, it will be determined if the application of a new thermo-ecological criteria can serve as a more practical alternative to traditional optimization methods, as this will determine the existence of a compromise between efficiency and cooling capacity.

As previously mentioned, an indirect-fired, single effect absorption chiller has four main components in which the heat transfers take place; these are the generator, condenser, evaporator and absorber. A basic schematic diagram of this type of absorption chiller is depicted in figure 2.

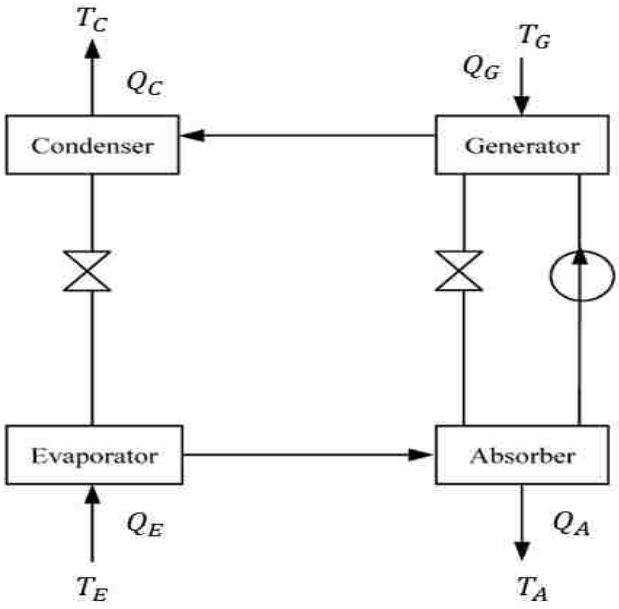

*Figure 2: Single-Effect Absorption Refrigeration Cycle. The components that constitute an absorption refrigeration system are; a generator, an absorber, an evaporator and a condenser. (*Chen, J. et al 1998)

The working fluid running in the system is made of a refrigerant and a solution that absorbs refrigerant. Refrigerant vapor comes from the evaporator and goes to the absorber, where it is absorbed in a liquid. The liquid is then sent to the generator where the refrigerant is boiled out of the solution, by taking the generator's heat reservoir. The solution and refrigerant are then sent to the condenser where heat is rejected to the environment. Finally, working fluid comes back to the evaporator, and the cycle is completed (Acikkalp, E. et al 2013). In other words, heat energy Q_G is supplied from the heat source at a high temperature T_G to the generator, where the working fluid is concentrated in the absorbent by evaporating the working medium. The weak solution passes through a valve into the absorber. The working medium is then condensed in the condenser and subsequently transferred to the evaporator. In such process, the amount of heat Q_C is released from the condenser to one heat reservoir at temperatureT_C. The liquid working medium is evaporated due to the additional

heat Q_E from the cooled space at a low temperature T_E to the evaporator. The vaporized medium is then transferred to the absorber where it is absorbed by the weak solution and the amount of heat Q_A is released from the absorber to the other heat reservoir at temperatureT_A. The strong solution produced in the absorber is pumped into the generator. The working fluid is transferred around the system by a solution pump. The work input required by such solution pump is negligible relative to the energy input to the generator and is often neglected for the purpose of analysis (Chen, J. et al 1999).

In figure 2, the absorber-generator assembly is the heat engine part, and similarly, condenser-evaporator assembly is the refrigeration part. The output power of the generator-absorber assembly, which can be considered to be a virtual heat engine, is used as the input power to the evaporator-condenser assembly (Bhardwaj, P. K. et al 2003). Real absorption refrigerators, as the one depicted in figure 2, usually suffer from a series of irreversibilities. These include the irreversibility of the finite-rate heat transfer and the internal irreversibilities resulting from the friction, eddies, mixing and other irreversible effects inside the working substance each of which can in principle decrease the efficiency of the refrigerator systems (Chen, J. et al 1999). Various studies focused on the irreversibilities mentioned here have been conducted and the methods and results of such studies will be explored further in sections 2.2 – 2.7.

2.0 Back ground and literature review

2.1 Background

A four-temperature-level absorption chiller is a complex device and its performance is affected by different irreversibilities (both external and internal). If all of the individual

irreversibilities affecting the device were taken into account, calculating the system's performance would be quite difficult if not impossible. Because of this and in order to obtain some significant analytical solutions of the key performance parameters, much of the research that has been done has establish a simplified cycle model which can reveal the main performance characteristics of a four-temperature-level absorption refrigerator (Chen, J. et al 1999).

2.2 Literature review

In the following sections a review of reports and research documents regarding the analysis and optimization of absorption chillers is presented. These sources will serve as the foundation to develop a mathematical model that will be used to analyze the system's performance. The analyses and the results of such are discussed in sections 3 and 4.

2.3 Energy-Exergy balances: An overview

The continuous increase in the cost and demand for energy has led to extensive research and development for utilizing available energy resources efficiently by minimizing waste energy (Abdulateef, J. M. et al 2012). Operating on low-grade energy and being environmentally friendly, absorption refrigeration systems have received a lot of attention and many research and development efforts have been dedicated to this type of systems. An absorption refrigerator is a heat operated refrigeration machine that operates on one of the earliest known principles of refrigeration (Farshad, P. Z. et al 2011). The single effect absorption chiller has been the most outstanding for research and development. It is important to note that system performance can be enhanced by reducing the irreversibility losses in the system by using the principles of the second law of thermodynamics. The

second law of thermodynamics has established that entropy generation minimization is an important technique to achieve optimal system configuration and better operating conditions (Abdulateef, J. M. et al 2012). Along with the minimization of entropy generation, the second law of thermodynamics has been implemented to provide a better understanding of the thermal performance characteristics of each component in the system. This law also helps to identify the component with high energy dissipation and irreversible losses. This in turn allows focusing more attention to such component in order to investigate and reduce its irreversibility losses.

As it is known, energy can be transformed from one form to another while its quality changes. According to the first law of thermodynamics, the magnitude of energy is conserved in a process. However, from experimental evidence, loss of the quality of energy usually causes the outlet energies to have a lower value compared to the inlet energies during any process. The main goal of an energy analysis is to determine the balance of different forms of energy for a particular system. On the other hand, energy analysis does not indicate how the energy transforms (such as heat transfer) or the locations where energy degrades due to entropy production and exergy destruction.

Exergy (the maximum theoretical useful work) is a principle for measuring the working ability of different energies. An opportunity for doing useful work exists when two systems at different states are placed in communication, for in principle, work can be developed as the two are allowed to come into equilibrium. Alternatively exergy can be defined as the minimum theoretical useful work required to form a quantity of matter from substances present in the environment and to bring the matter to a specified state (Bejan, A. et al 1996). Exergy is a measure of the departure of the state of the system from that of the

environment. It is therefore an attribute of the system and environment together. Exergy can be destroyed and generally is not conserved. Due to thermodynamic irreversibilities, the exergy efficiency of a process can be low in spite of a high energy efficiency, which indicates the quality degradation of different energies (Farshad, P. Z. et al 2011; Bejan, A. et al 1996).

Using the thermodynamic properties of the working fluid at different operating conditions, the authors of (Abdulateef, J. M. et al 2012) calculated the entropy generation of each component, the total entropy generation as well as the COP of an absorption refrigeration system. The model analyzed in (Abdulateef, J. M. et al 2012) is similar to the model presented in section 2.1 figure 2. It is a four-temperature-level single effect absorption refrigeration system. In the model, Q_{gen} is the heat input rate from the heat source to the generator, Q_{cond} is and Q_{abs} are the heat rejection rates from the condenser and absorber to the heat sinks, respectively. Subsequently Q_{evap} is the heat input rate from the cooling load to the evaporator.

The performance equations of the components, considering continuity (mass balance), the first law of thermodynamics (energy balance), and the second law of thermodynamics (entropy generation) used in (Abdulateef, J. M. et al 2012) are the following:

- Mass balance

$$\Sigma_e(\dot{m}_e) = \Sigma_i(\dot{m}_i) \quad (1)$$

- Energy balance

$$\dot{Q}_k = \Sigma(\dot{m}_e * h_e) - \Sigma(\dot{m}_i * h_i) \quad (2)$$

- Entropy balance

$$\dot{s}_{gen,k} = \Sigma(\dot{m}_e * s_e) - \Sigma(\dot{m}_i * s_i) - \frac{\dot{Q}_k}{T_k} \quad (3)$$

Where Q_k is the heat added to the component k at temperature T_k. T_k is the entropic average temperature at which heat flows across the component. $\dot{S}_{gen,k}$ is the entropy generation of component k of the system (Abdulateef, J. M. et al 2012). Employing the equations presented above and the given parameters, the thermodynamic properties of the fluid at all reference points in the cycle were calculated. Simulations were performed in which internal component temperature variations were carried out (temperatures in the generator, evaporator, absorber and condenser were varied). Results of the simulations were represented graphically in (Abdulateef, J. M. et al 2012).

Such results show the effects the temperature variations of heat reservoirs (generator, evaporator, absorber and condenser) have on the COP and entropy generation of the system. It was concluded that the second law analysis provided and alternative view of system performance and supplied information regarding how losses of different components can be quantified and where a given system should be modified for best performance. It was also determined that the thermodynamic properties of the working fluid are key factors to determine the entropy generation of each component, the total entropy generation and the COP of an absorption refrigeration system. The results show that an increase in the generator temperature causes an increase in the COP. From the results it appears that the COP is more sensitive to changes in the operating conditions of the generator and the evaporator or any other component that affects them. On the other hand, the total entropy generation considers the effect of all the system components (Abdulateef, J. M. et al 2012).

A similar analysis as the one presented in (Abdulateef, J. M. et al 2012) was conducted by (Farshad, P. Z. et al 2011). Here, a closer look at the effect of temperature variations to the working fluid in the internal components of a four-temperature-level absorption chiller is observed and analyzed. In this analysis, the authors consider the first law of thermodynamics in order to determine the energy balance of the system. The second law of thermodynamics was employed to determine the heat transfer along with the entropy generations of each component. The analysis performed in (Farshad, P. Z. et al 2011) was more extensive in the sense that the authors calculated the exergy destruction at each of the components of the system, which in turn allowed determining the exergy balance. In order to determine the exergy destruction in each of the system components, it was necessary to define the enthalpies and entropies at the inlets and outlets of such components. The exergy of a fluid stream (or exergy stream) can be defined as in (Medrano, M. et al 2010):

$$\psi = (h - h_o) - T_o(s - s_o) \tag{4}$$

Where ψ is the physical exergy of the fluid (or exergy stream) at temperature T, the terms $h\ and\ s$ are the enthalpy and entropy of the fluid. Whereas $h_o and\ s_o$ are the enthalpy and entropy of the fluid at the environmental temperature T_o and standard atmospheric pressure P_o.

The exergy transfer to a steady flow system is equal to the exergy transfer from it plus the exergy destruction within the system. The exergy balance for the steady flow system from (Farshad, P. Z. et al 2011) can be represented as follow:

$$\Sigma_i \dot{Q}\left(1 - \frac{T_o}{T}\right) - \Sigma_e \dot{Q}\left(1 - \frac{T_o}{T}\right) - \dot{W} + \Sigma_i \dot{m}\psi - \Sigma_e \dot{m}\psi - \dot{E}_{des} = 0 \tag{5}$$

In equation 5, the first and second terms represent the exergies associated with the heat transferred from the source maintained at a temperature T. The third term is the exergy of mechanical work added by the solution pump to the control volume, which usually is considered to be negligible. This is because in absorption chillers, the solution pump has a very low input power requirement. The fourth and fifth terms are the exergies of the inlet and outlet streams of the control volume. The last term is the exergy destruction that takes place in the control volume. Another efficiency used in their studies is that of exergy, simply known as the exergetic efficiency (E_COP), which is defined as the ratio of the useful exergy obtained from a system to that which is supplied to the system.

Once the thermodynamic equations were established, the entropies, enthalpies, heat transfers and exergy transfers for each of the components were calculated. These values were calculated through the variation of the component's inlet temperatures and by assuming no pressure drops. Results of some of the temperature variations were presented in (Farshad, P. Z. et al 2011). These results show that the exergy loss of the generator increases as the generator inlet temperature is increased. For the same variation, the COP slightly increases while the E_COP decreases. Lastly, the COP increases while the E_COP decreases when the evaporator inlet temperature is increased (Farshad, P. Z. et al 2011).

From these results, it was concluded that in spite of relatively high energy efficiency, the absorption chiller has low exergy efficiency. Also, it was mentioned that the exergy loss that occurred in the generator was a considerable fraction of the overall exergy loss of the system. From this, the authors determined that the generator is the most important component of the absorption chiller and that it has a greater effect on the COP and E_COP of the system. The second important component in the system is the absorber. Finally, it was stated that the

performance of the absorption chiller is strongly influenced by the operating temperatures of each component. It is important to note that in their analysis (Farshad, P. Z. et al 2011) the authors performed an energy and exergy analyses where neither heat leaks nor internal irreversibilities were accounted for.

2.4 Finite-time thermodynamics method: a brief description

Finite-time thermodynamics deals with the fact that there must be a finite temperature difference between the working fluid and the source/sink heat reservoirs (with which it is in contact) in order to transfer a finite amount of heat in a finite time. Finite-time thermodynamics is concerned with how constrains on time (or rate) affect the performance of a system (Andresen, B. et al 1984). The concept of finite-time thermodynamics started with the work of Curzon-Ahlborn, when they considered a simplified model of a Carnot cycle between reservoirs, in which there is only the irreversibility of heat transfer (Curzon, F. L., Ahlborn, B. et al 1975; Bhardwaj, P. K. et al 2003). The finite time thermodynamic optimization of refrigerators coupled with infinite heat capacity thermal reservoirs has been determined by various researchers (Chen, J. et al 1995; Chen, J. et al 1997; Chen, J. et al 1998; Davis, G. W. et al 1997; Yan, Z. et al 1989; Chen, J. et al 1995; Wu, C. et al 1993). However, it is often the case in practice that the cooling load is generated from heat that is transported by a finite amount of material with finite heat capacity, rather than from heat extracted from an isothermal infinite reservoir. With finite-time thermodynamics and the ideas mentioned in (Curzon, F. L., Ahlborn, B. et al 1975), studies on the optimization of endoreversible refrigerators have been conducted.

Endoreversible refrigerators are systems that consider only finite-rate heat transfer losses or merely external losses (K. C. Ng. et al 1999). However, general irreversible cycles include finite-time heat transfer, heat leakage and irreversibilities due to the internal dissipation of the working fluid, as mentioned in section 2.1. In many studies, such irreversibilities have been established and accounted for in order to analyze the optimum performance of irreversible, heat energy driven refrigerators and heat pumps (K. C. Ng. et al 1999; Chen, J. et al 1997; Chen, J. et al 1995). In most of these studies, to simplify the complexity of the system's internal operations while accounting for the various types of irreversibilities (finite-time heat transfer & heat leakage), internal irreversibilities are included in the analysis by introducing an internal irreversibility factor, which is defined by the second law of thermodynamics (Wu, C. et al 1992). In finite-time thermodynamics the absorption refrigeration system can be considered as a combined cycle, consisting of a heat engine and a refrigerator, having non-uniform heat sink/source temperatures but uniform component temperatures (Chen, J. et al 1995; Yan, Z. et al 1989). In most of the studies, however, it has been assumed that the heat sink/sources are uniform. This assumption was made to simplify the analysis of the external irreversibility of finite-time heat transfer with the surroundings. The case of non-uniform sink/source temperatures will be explored in sections 3 and 4.

2.5 Absorption refrigeration system: irreversible, four-temperature-level.

A theoretical analysis and optimization of a four-temperature-level irreversible absorption chiller was conducted in (Chen, L. et al 2006). In the analysis, the external and internal irreversibilities of the system were accounted for utilizing the methods described in section 2.4. The goal of this study was to derive and determine the coefficient of performance

(COP) and the cooling load, the maximum COP and the corresponding cooling load, and the maximum cooling load and the corresponding COP of the cycle. The system model was coupled to constant-temperature heat reservoirs. The system model employed in the study was similar to the one presented in figure 2. Also, in (Chen, L. et al 2006) the system was simplified in order to account for its internal irreversibilities and the heat leak to the environment.

The authors assumed a steady state operation, having the working fluid inside the different components exchange heat with the heat reservoirs at temperature $T_H, T_L, T_o,$ $and\ T_M$ (heat reservoir interacting with the generator, evaporator, condenser and absorber respectively) during the full cycle time. The corresponding working fluid temperatures in the internal component are $T_1, T_2, T_3 and\ T_4$ (generator, evaporator, condenser and absorber). Utilizing the first law of thermodynamics and using the information provided in their system diagram, the authors determined that:

$$Q_1 + Q_2 - Q_3 - Q_4 = 0 \quad (6)$$

Where $Q_1, Q_2, Q_3\ and Q_4$ are the heat transfers into and from the generator, evaporator, condenser and the absorber. It was assumed that the heat transfers between the working fluid in the heat exchangers and the external heat reservoirs were carried out under a finite temperature difference. The heat exchanges are assumed to be isothermal and the equations of such are:

$$Q_1 = (U_1 * A_1)(T_H - T_1) \quad (7)$$

$$Q_2 = (U_2 * A_2)(T_L - T_2) \quad (8)$$

$$Q_3 = (U_3 * A_3)(T_3 - T_o) \quad (9)$$

$$Q_4 = (U_4 * A_4)(T_4 - T_M) \quad (10)$$

$$Q_L = K_L(T_M - T_L + T_o - T_L) \quad (11)$$

In equations 7 to 11 the terms $U_1, U_2, U_3\ and\ U_4$ are the overall heat-transfer coefficients of the generator, evaporator, condenser and absorber respectively. K_L is the heat leak coefficient. $A_1, A_2, A_3 and\ A_4$ are the heat-transfer surface areas of the generator, evaporator, condenser and absorber respectively. The total heat-transfer area is defined by:

$$A = A_1 + A_2 + A_3 + A_4 \quad (12)$$

In addition an optimization parameter was defined as the ratio of the heat transfer between the condenser and the absorber (Chen, L. et al 2006) as the parameter *a*:

$$a = \frac{Q_4}{Q_3} \quad (13)$$

Note that the equations presented in this section are the general equations that have been most regularly employed in studies pertaining to the performance optimization of absorption chillers. As mentioned in section 2.3, real absorption chillers are complex devices and suffer from a series of irreversibilities. Finite-time heat transfer irreversibilities and heat leakages affect the overall performance of the system. Along with these, the internal dissipation of the working fluid is another main source of irreversibility which contributes to the decrease of COP and cooling load of the system (Chen, L. et al 2006).

Utilizing the second law of thermodynamics, the irreversibility factor *I* used to describe the irreversibility due to internal dissipation of the working fluid can be introduced as:

$$I = \frac{(\frac{Q_3}{T_3}+\frac{Q_4}{T_4})}{(\frac{Q_1}{T_1}+\frac{Q_2}{T_2})} \ , \ I > 1 \qquad (14)$$

When the influence of the internal irreversibilities of the working fluid is negligible, I = 1, the cycle of the working fluid is endoreversible; when I >1, the cycle of the working fluid is irreversible. The internal irreversibility factor has been used frequently in various studies and considerably simplifies the second law analysis. From the model and the second law of thermodynamics it was determined that:

$$\frac{Q_1}{T_1} + \frac{Q_2}{T_2} - \frac{Q_3}{IT_3} - \frac{Q_4}{IT_4} = 0 \qquad (15)$$

By employing equations 6 to 15 along with mathematical methods and manipulations, the authors conducted a series of numerical analyses in order to determine the fundamental optimal relation between the coefficient of performance and the cooling load. They used the standard definitions of the COP and the cooling load of an absorption chiller, given by:

$$\varepsilon = \frac{Q_2 - Q_L}{Q_1} \qquad (16)$$

$$R_\varepsilon = Q_2 - Q_L \qquad (17)$$

The cooling load of absorption refrigerators is always smaller than Q_2 due to the heat leak between the system and the environment reservoirs to the cooled space (Chen, L. et al 2006).

From their analysis, the relation between the standard COP and the cooling load was derived. Also, the relation of the maximum COP and the corresponding cooling load were derived (Chen, L. et al 2006). The results obtained are shown in figure 3, which displays the relationships between the COP and cooling load.

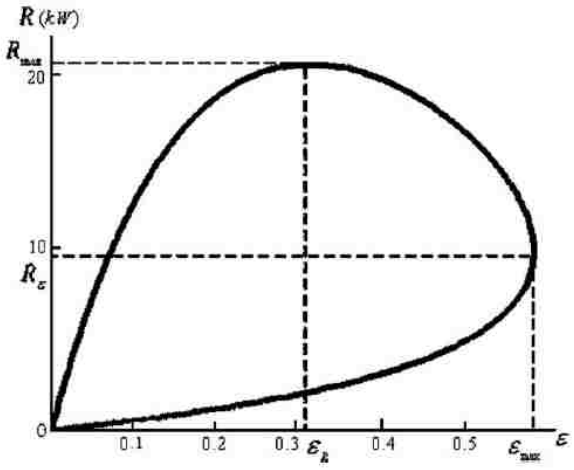

Figure 3: The optimal COP vs. the cooling load R from (Chen, L. et al 2006)

In figure 3, it is suggested that the optimal operating region of an absorption refrigerator should be the part of the curve with a negative slope. In this zone, the COP will increase while the cooling load decreases and vice versa. From these results, an optimization method is suggested by performing a distribution of the heat exchanger total inventory. This means that both the heat-transfer coefficients and areas will be varied to obtain the optimal distribution relation of the heat conductance in the system (Bejan, A. et al 1995; Chen, L. et al 2006). The authors explained, that for a fixed value of *I*, R_{max} , ε_R, ε_{max}, and R_ε decrease with the increase of *a*, and with a fixed value of *a*, R_{max} , ε_R, ε_{max}, and R_ε decrease with the increase of *I*. The results show that the internal irreversibility factor has a significant impact

on the system's performance. Similar results are obtained in this study and are presented in section 4.

The article presents several cases in which input parameters are varied. The parameters varied in such cases include the internal irreversibility factor I, the heat reject distribution parameter a, the heat leak coefficient K_L, the heat reservoir temperatures ($T_H, T_M, T_o \& T_L$), the overall heat-transfer coefficients and the heat-transfer surface areas (Chen, L., Sun, F. et al 1996; Chen, L., Sun, F., Wu, C. et al 2001; Gordon, J. M., Ng, K. C. et al 2000; Goth, Y., Feidt, M. et al 1986; Wijeysundera, N. E. et al 1999; Yan, Z et al 1990; Chen, J. et al 1999). These cases, describe the effects on the system's outputs depending on the type of variation.

In summary, (Chen, L. et al 2006) analyzed and optimized the performance of a four-temperature-level, irreversible absorption refrigeration cycle, taking into account the heat resistance, heat leakage, and internal irreversibility losses. Detailed numerical examples were derived and used to determine the effects that the system parameters had on the COP and cooling load. These results have realistic significance and may provide new theoretical guidance for the performance improvement and optimization of absorption chillers. Some of the parameters and methods used in this analysis will be further explored and employed in a second law analysis presented in sections 3 and 4.

2.6 thermodynamic modeling of absorption chillers

The authors of (Ng, K. C. et al 1999) explain and explore the ideologies that have been used in previous absorption chillers studies. They point out that many of the previous studies are far from accurate as these are focused on models that have been analyzed only

from a finite-time-thermodynamics point of view. According to the authors, the problem with this type of approach is that the model is assumed to be an endoreversible system, which is not how actual systems behave. They also mention that these models only consider finite-rate heat transfer as the only irreversibility. However, the behavior of real chillers is governed by external and internal dissipative losses, as well as heat leaks from all processes in the system. As a consequence, the study predicts that the coefficient of performance (COP) decreases monotonically as the cooling rate of the system increases.

In their paper, the authors consider a four-heat-reservoir model, which presumably follows the behavior of real absorption chillers in which the absorber and condenser temperatures are different (Chua, H. T., Qian, H. et al 1996; Chua, H. T., Ng, K. C. et al 1997)**.** In this study, the absorption chiller thermodynamic model deals with external losses due to finite-rate heat transfer, internal dissipative losses and heat leaks in the system, similar to the model mentioned in sec 2.4. The thermodynamic model employs the basic laws of thermodynamics and makes no unnecessary constrains, as done in some of the endoreversible models. The authors emphasize that the model employed differs from endoreversible models in that it considers the case with substantial internal heat leaks between the internal chambers, mainly from generator to condenser and absorber to evaporator (Ng, K. C. et al 1999). On the other hand, significant external heat leaks to or from the environment are accounted for at the generator and evaporator only. The model used in the analysis is a single-stage absorption chiller which employs thermal energy as the driving force. It interacts with four temperature reservoirs and works at steady state. Once the model and its operating conditions were defined, it was compared to an experimental facility to show that the true absorption chiller behavior is governed by finite-rate heat transfer losses, internal dissipation

losses, and heat leaks. The results of the comparison of theory and experiment studies obtained by the authors are presented in (Ng, K. C. et al 1999).

Table 1 in (Ng, K. C. et al 1999) displays the measured results obtained by employing data presented in (Manual for single-stage abs. chiller 1995). From the variation of the inlet temperatures of the evaporator, generator and condenser; the heat transfers ($Q_e and\ Q_a$), COP and heat rejection ratio Ξ were calculated by employing equations similar to the equations introduced in section 2.4. The variable Ξ, is a dimensionless parameter which indicates the ratio of heat rejection via the absorber to the total heat rejection of the system. Table 2 of (Ng, K. C. et al 1999) gives the estimated values of the system at various coolant and heat source temperatures. For the results in (Ng, K. C. et al 1999), the internal dissipative losses and the thermal conductance terms were computed based on the internal temperatures of the heat exchangers.

From their analyses, the authors concluded that the simple thermodynamic model employed accurately captures the key dominant losses that govern the performance of a four-heat-reservoir, single effect absorption chiller. The model takes into consideration the key losses, namely, finite-rate heat transfer, internal dissipative and heat leaks losses (it is important to note that even though a heat leak loss is mentioned in the article, there is no mathematical representation of such when the heat transfers in the system were defined). According to the results obtained, it was stated that the thermodynamic model provides better insight for understanding chiller behavior over a wide span of operating conditions, since the model used in the analysis is generic and applies to all absorption chillers. With some of the results obtained in this study taken into account, a detailed examination of a four-temperature-level absorption chiller is presented in sections 3 and 4.

2.7 Thermo-ecological criterion and methods for optimization

An ecological criterion is another optimization method that serves to identify the heat engine configuration that makes the best compromise between power output and lost power. It is also an important method employed to represent the best mode of operation of a system, especially that of an endoreversible Carnot engine. The first to propose this criterion was Angulo-Brown in (Angulo-Brown, F. et al 1991). Such optimization criterion follows the work performed by Curzon and Ahlborn (Curzon, F. L., Ahlborn, B. et al 1975), which is the pioneering work that established more realistic theoretical bounds on entropy producing thermodynamic processes. In short, the purpose of the ecological criterion is to include the entropy generation of the system into the system's optimization. The criterion is shown as:

$$\dot{E} = \dot{W} - T_L \dot{\sigma} \tag{18}$$

Where, $\dot{\sigma}$ is the rate of entropy production of the system while T_L represents the temperature of the cold reservoir. The criterion however, was demonstrated to be more suitable if the ambient temperature T_o is used instead of the cold reservoir temperature T_L (Acikkalp, E. et al 2013).

A modified ecological optimization was employed in order to provide the maximum cooling load, minimum operation input and minimum entropy production in the system (Acikkalp, E. et al 2013). The method shown seeks to provide a more effective operation of absorption refrigerators by employing the modified ecological function, along with the first and second law of thermodynamics. In their study, a four-temperature-level absorption chiller which interacts with infinite heat capacity reservoirs was analyzed (Acikkalp, E. et al 2013). This system had two main parts: the refrigeration part (condenser-evaporator) and the

heat engine part (absorber-generator). The internal irreversibilities, as in the case of section 2.4, where represented by a parameter I in an effort to simplify the complexity of the overall system. The heat transfers in each of the heat exchangers were calculated using initial values for the temperatures in the heat reservoirs, surface areas, internal irreversibility factors, heat transfer surface area factors and working fluid temperature ratios (Acikkalp, E. et al 2013).

Through mathematical manipulation and substitution, the authors calculated the working fluid temperatures in each of the absorption chiller components. These were then utilized to calculate the maximum cooling load as well as, the maximum power output and the maximum exergy destruction of the system. Once the mathematical representation for the system was obtained, parameter variations were performed and the effect such variations had on the performance (ecological function, exergy destruction, COP, cooling load) of the system were recorded. A variation of the working fluid temperature in the absorber causes the ecological function and the exergy destruction to decrease while the COP increases. Meanwhile, a variation of the working fluid temperature in the generator has the opposite effect. Also, a variation of the working fluid temperature inside the condenser decreases the value of the ecological function, the exergy destruction, the cooling load and the COP. Variations of the working fluid temperature inside the evaporator have the opposite effect (Acikkalp, E. et al 2013).

Once the results of the variations were obtained, it was concluded that a balance between the cooling load, the load supplied to the system, and entropy production was established. However, the optimization did not account for the losses due to heat leakage, which should be an important factor in this type of analysis.

Similar optimization analyses were performed by Huang and Kang (Huang, Y. et al 2008). In these, an ecological criterion for the best mode of operation of the four-temperature-level absorption heat-pump cycle was introduced. The analysis and optimization is performed assuming a linear heat-transfer law. As in the previous example (Acikkalp, E. et al 2013) the authors of (Huang, Y. et al 2008) accounted for the losses of heat resistance (finite-rate heat-transfer) and internal irreversibilities, but excluded losses due to heat leaks. Variations of the inlet temperatures on the heat reservoirs were performed, and the effect these variations had on the heating load, ecological criterion, and coefficient of performance were recorded. It was concluded that the optimal relation of the heating load, the coefficient of performance and the total heat-transfer area was achieved. It was also concluded that the optimization of the ecological function made the entropy production rate of the cycle decrease, while the coefficient of performance increased with the cost of an appropriate decrease in the heating load. Although the analysis presented pertains to an absorption heat pump, the same approach can be applied to an absorption refrigerator (Huang, Y. et al 2008).

Wouagfack and Tchinda also conducted an investigation regarding the performance optimization of irreversible refrigerators based on a thermo-ecological criterion (Wouagfack, P. A., Tchinda, R. et al 2011). In this paper, an optimization study of an irreversible refrigeration absorption system was presented. For the analysis, the ecological coefficient of performance (ECOP) was the objective function of the system. For the performance optimization, the effects of finite rate heat transfer, heat leakage and internal irreversibilities were taken into account. For simplicity, the second law of thermodynamics was employed in order to introduce a parameter used to represent the total internal irreversibilities of the system and thus decrease the level of its complexity. The coefficient of performance, specific

cooling rate and specific rate of entropy production were obtained from the standard definitions and analytical calculations. By employing the before mentioned parameters and with the definition of the general thermo-ecological criterion function in (Wouagfack, P. A. et al 2011) the new ecological coefficient of performance (ECOP) of an absorption refrigeration can be written as:

$$ECOP = \frac{\dot{Q}_E - \dot{Q}_L}{T_{env}\dot{\sigma}} \quad (19)$$

Where $\dot{Q}_E$ represents the rate of heat transfer in the evaporator side of the absorption chiller, $\dot{Q}_L$ is the rate of heat leakage from the heat sink, T_{env} is the ambient temperature and $\dot{\sigma}$ is the overall entropy production of the system. Following several mathematical processes, the authors arrived at the maximum ecological coefficient of performance (ECOP_max), temperature of the working fluid, rate heat transfers and temperature ratios. From these results, the authors implemented parameter variation (heat leakage coefficient, internal irreversibility and source temperature ratio) and recorded the effects such variations had on the ECOP and the specific entropy production rate. From the results obtained and shown in figure 5 of (Wouagfack, P. A. et al 2011) the authors concluded that the ecological performance of the irreversible absorption refrigerators have been optimized by considering the new thermo-ecological criterion as the objective function. The objective function, coupled with the first and second law of thermodynamics, is the ecological coefficient of performance (ECOP) and is defined as the cooling load per unit loss rate of availability. The optimum performance parameters, such as the specific cooling rate, the specific entropy generation rate, the heat-transfer area distribution, the internal working fluid temperatures,

and the coefficient of performance were obtained analytically through the maximization of the defined thermo-ecological objective function for an irreversible absorption refrigerator.

It is also mentioned that the effects of the internal irreversibility, the heat leakage coefficient and the source temperature ratio on the global and optimal ECOP performances were examined (Wouagfack, P. A., Tchinda, R. et al 2011). It was also shown that the maximum coefficient of performance (COP) and the ecological coefficient of performance (ECOP) occurred for the same operating conditions in spite of their different meaning, as the COP takes into account only the first law of thermodynamics and the ECOP takes into account both the first and second law of thermodynamics. The relationship between the COP and ECOP is presented as:

$$ECOP = \frac{T_{C^*}\, COP}{T_{env}(1-\tau)(COP-\varepsilon_r)} \qquad (20)$$

A similar approach of the ECOP, as the one presented in (Wouagfack, P. A. et al 2011), will be used in the analysis of a four-temperature-level irreversible absorption chiller presented in sections 3 and 4.

3.0 Purpose and methodology

3.1 system description

The system analyzed is a four temperature level absorption chiller, for which two types of heat exchange analyses were performed. The analyses are that of infinite heat capacity in the heat reservoirs (constant temperature throughout the reservoirs in the cycle) and finite heat capacity in the heat reservoirs (temperature difference between inlet and outlet in the heat reservoirs throughout the cycle). The assumptions for the system are the following:

1. Steady state operation
2. Pump power input is negligible (no power input)
3. Well insulated internal components
4. Working fluid temperature is uniform (but differs from component to component) through each of the system's components.
5. Air is the fluid used for the heat exchanger interactions (outer components) and is defined through the Engineering Equation Solver (EES) software as an ideal gas (Klein, S. A et al 2006).
6. Standard atmospheric pressure is assumed in the cycle.
7. Pressure drop across all heat exchangers is negligible.

A schematic of the system, with infinite and finite heat capacity reservoirs is presented in figure 4. The system shares the characteristics of all absorption chillers in that it is consists of four main components, the generator the evaporator, condenser and the absorber.

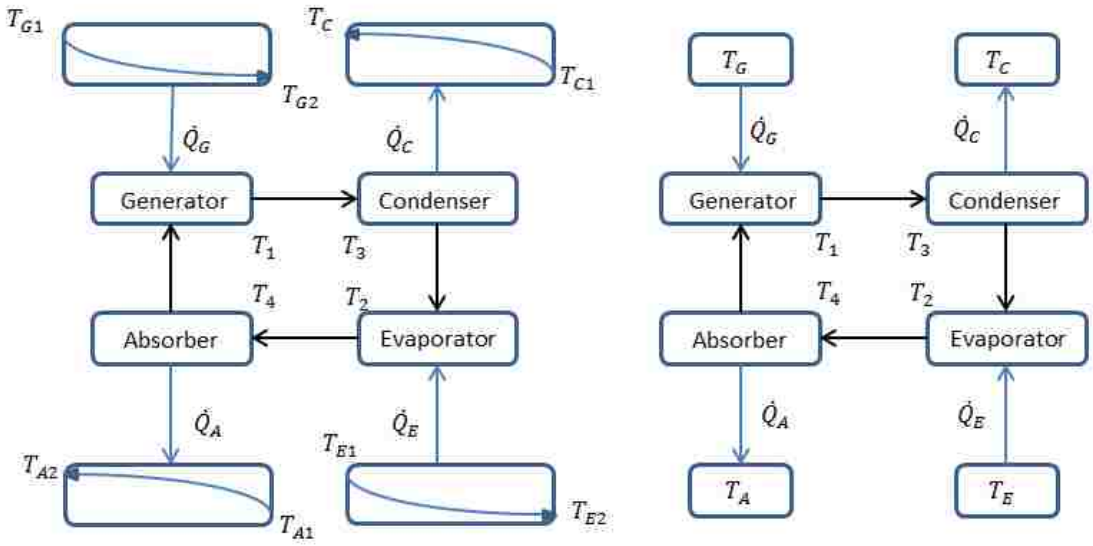

Figure 4: Absorption chiller schematics a) finite heat capacity reservoirs and b) infinite heat capacity reservoirs.

The models shown in figure 4 follow the general layout of an absorption chiller. For both models in figure 4 the arrows inside the absorption chiller represent the direction in which the working fluid moves. Also, the arrows coming from and going into the heat reservoirs indicate the direction of the heat transfer (into or out of the absorption chiller). The differences between the models a) and b) in figure 4**,** are that model a) interacts with finite heat capacity reservoirs, for which temperature variations are represented by gradient arrows. On the other hand, model b) interacts with infinite heat capacity reservoirs. As stated in the previous assumptions, the work input required by the working fluid pump is negligible relative to the energy input of the generator and evaporator, in an effort to simplify the analysis of the models. Consequently the pump work is neglected as per the explanation in section 2.1. It is also assumed that the working fluid temperature is uniform throughout each of the system's components (generator, evaporator, condenser & absorber).

3.2 Purpose statement

The goal of this study is to perform a second law analysis to investigate and quantify the compromise between the total efficiency (COP) and cooling load for a four temperature level absorption chiller, taking into account the irreversibilities due to finite time heat transfer, heat leakage and internal fluid dissipations. Once a mathematical model that accurately represents the system is developed, some of the system's parameters will be varied in an effort to determine the best operational parameters. This is done to gain some insight for future research and optimization for this type of system. The performance of the system will be quantified through common effectiveness measurements of energy utilization such as energy and exergy efficiencies. Special attention will be dedicated to entropy production and exergy destruction and how these two parameters affect the overall performance (e.g. COP

and cooling capacity) of the system. Along with these methods, a new thermo-ecological function will be implemented to the analysis to determine the best operating conditions for the system.

3.3 Methodology of analysis

A first and second law of thermodynamics analysis will be implemented on the system using the computer software EES. The first and second laws are employed in order to verify that the model presented in EES follows an adequate thermodynamic behavior and proper performance. For each calculation the conservation of energy and the balance of exergy are calculated to make sure the first law and the second law of thermodynamics are not violated. For the heat transfers that take place in the heat reservoirs, it is assumed that the fluid utilized is air, which is taken from EES as an ideal gas. Also, the internal pressure in all of the components is assumed to remain constant at 1 ATM. The system has multiple control parameters which will be varied and explained in the upcoming sections.

EES is an equation-solver computer program. It solves systems of equations (i.e., relationships between variables) automatically, which frees the user from having to develop their own iterative technique for solving a set of non-linear equations. There are many additional features associated with EES; for example such as unit checking, optimization, numerical integration, high quality property data, plotting and uncertainty analyses. EES also provides many built-in mathematical and thermophysical property functions useful for engineering calculations (Klein, S. A et al 2006).

3.3.1 System's control parameters

The performance of the system will be observed and compared at different operating conditions. In order to perform such comparisons it will be necessary to execute parameter variations and record how sensitive the system is to these variations. A list of the system controls parameters is presented in table 1, including the ranges each of the parameters will be varied for. In this section, the reasons for selecting such ranges will be explained.

Input Parameters	Unit	Symbol	Value		
			Minimum	Maximum	Nominal
Inlet temperature of heat reservoir interacting with the Generator	K	T_{G1}	400	450	410
Inlet temperature of heat reservoir interacting with the Evaporator	K	T_{E1}	275	298	283
Inlet temperature of heat reservoir interacting with the Condenser	K	T_{C1}	300	340	333
Inlet temperature of heat reservoir interacting with the Absorber	K	T_{A1}	300	330	313
Heat exchangers surface areas (for each HX)	m^2	A	0	1200	300
Working fluid temperature inside of the Generator	K	T_1	385	400	390
Absober/Condenser heat reject ratio "a"		a	0.5	2	1.4
Internal irreversibility factor		I	1	1.1	1.05
Heat leak coefficient	$\frac{kW}{K}$	K_L	0	15	4
Effectiveness of heat exchanger		eff	0.25	0.9	0.75
Overall heat transfer coefficient (for the heat exchangers)	$\frac{kW}{m^2K}$	U	0	4	2.5

Table 1: Input parameters

Table 1 contains the main input parameters that will be varied in order to record the effects these variations have on the system's overall performance. The inlet temperatures of the heat reservoirs have been selected based on the literature in sections 2.3-2.7. The nominal values presented in table 1 are the values that have been used in many of the studies presented in the literature review section.

From table 1, the input parameters that are of highest importance are the inlet temperature of the heat reservoir interacting with the generator, the working fluid temperature inside the generator (because the remaining working fluid temperatures depend on this temperature to be calculated), the heat exchanger surface areas and the heat transfer coefficients. Results obtained from the simulations of the variations of some of these parameters will be shown in upcoming sections.

3.3.2 Evaluation Metrics

Common thermodynamic metrics are used to evaluate the system's performance under different operating conditions. As before stated, the first and second laws of thermodynamics will be employed in order to 1) ensure that the system follows an acceptable thermodynamic behavior and 2) to observe how sensitive the mathematical model is to the variations of input parameters.

From figure 4, the working fluid temperatures inside the components of the absorption chiller (for both infinite and finite heat capacity reservoirs) are T_1, T_2, T_3 and T_4 in the generator, evaporator, condenser and absorber respectively. The inlet temperature of the heat reservoirs are T_{G1}, T_{E1}, T_{C1} and T_{A1}. It is important to notice that the working fluid temperatures inside the components of the absorption chiller are of high importance as these

are employed to determine the heat transfers between the heat reservoirs and the components in the system. The rates of heat transfer between the heat reservoirs and the generator, evaporator, condenser and absorber are denoted by $\dot{Q}_G, \dot{Q}_E, \dot{Q}_C \; and \; \dot{Q}_A$, respectively.

Since one of the goals of this study is to quantify and compare the exergy destruction between the heat reservoirs and the internal components of the absorption chiller, the rates of entropy production and exergy destructions are calculated. Equations (3) and (5) serve to calculate such values and are modified for each of the cases described in section 3.1.

3.3.3 Analysis Procedure

The first approach consists of a four-temperature-level absorption chiller which interatcs with infinite heat capacity reservoirs. This model serves as a base model and it is similar to the examples presented in sections 2.2-2.7. The second approach consists of the same type of absorption chiller differing in that the heat reservoirs with which the system interacts have finite heat capacity for which an effectiveness-NTU method is used for the heat transfer analysis. The model used in the infinite heat capacity reservoir case, the effectiveness-NTU method and model in the finite heat capacity reservoir case are explained in sections 3.4, 3.5 and 3.6 respectively. Both models are evaluated and compared in sections 4.1 and 4.2 to observe the effects of the input parameter variations. The input parameter variations and results for the infinite heat capacity model are presented first and the finite heat capacity model are presented last. Along with the before mentioned methods, a new thermoecological approach is implemented to both models. This new approach is defined and explained in section 3.7.

3.4 Infinite Heat Capacity Model

For the first model (infinite heat capacity reservoirs), the heat transfer rate equations that will be employed in the heat balance of the absorption chiller can be written as:

$$\dot{Q}_G = (U_G * A_G)(T_{G1} - T_1) \quad (21)$$

$$\dot{Q}_E = (U_E * A_E)(T_{E1} - T_2) \quad (22)$$

$$\dot{Q}_C = (U_C * A_C)(T_3 - T_{C1}) \quad (23)$$

$$\dot{Q}_A = (U_A * A_A)(T_4 - T_{A1}) \quad (24)$$

$$\dot{Q}_L = K_L(T_o - T_{E1}) \quad (25)$$

Where $U_G, U_E, U_C and\ U_A$ are the overall heat transfer coefficients in$(\frac{kW}{m^2K})$ and $A_G, A_E, A_C and\ A_A$ are the heat transfer areas (m^2) of the generator, evaporator, condenser and absorber, respectively. $\dot{Q}_L$ & K_L $(\frac{kW}{K})$ are the leakage rate heat transfer and heat leakage coefficient of the system (for simplicity, it is assumed that in this particular case the heat leakage takes place between heat reservoir that interacts with the evaporator and the environment). Also, as explanied in section 2.2, in order to simplify the complexity of the internal irreversibilities in the components of the absorption chiller, a factor that represent these internal irreversibilities is introduced using equation (15). Equations (13), (16) and (17) are also employed in the analysis.

The energy balance of the system is achieved by a method similar to the one described by equation 6. The only difference is that the heat transfer due to the rate heat leakage will be included as:

$$E_{bal} = \dot{Q}_G + \dot{Q}_E - \dot{Q}_C - \dot{Q}_A - \dot{Q}_L \quad (26)$$

Equations (13, 15, 16, 17, 21-26) were used in conjuction to determine the heat transfers, coefficient of performance, cooling capacity, entropy production rates and exergy destruction rates of the system. For the last two items, the entropy prodution for this system is achieved by employing eq. (3), which is employed to calculate the individual rates of entropy production, and is written as:

$$\dot{\sigma}_{gen} = \Sigma_j \dot{\sigma}_j \quad (27)$$

Where $\dot{\sigma}_{gen}$ is the sum of the rates of entropy production between the heat reservoirs and the internal components of the absorption chiller. The individual rates of entropy production are calculated under steady state conditions with only heat transfer between the system and the thermal reservoirs. Using eq. (3) the rate of entropy production for each process can be writeen as:

$$\dot{\sigma} = -\Sigma_j (\frac{\dot{Q}_j}{T_j}) \quad (28)$$

Where the subscript j represents each component relation. The exergy destruction for this model is achieved by employing equation (5) which, with the assumptions of no exergy transfer by mass transfer and steady state operation can be written as:

$$\dot{E}_{des} = \Sigma_j \left(1 - \frac{T_o}{T_j}\right) \dot{Q}_j \quad (29)$$

Where the subscript j represents each individual exergy transfer between the heat reservoirs and the absorption chiller's components i.e. generator, evaporator, condenser and absorber.

3.5 Effectiveness-NTU method

The effectiveness-NTU method was used to model and evaluate the heat transfers which were used to determine the COP, R_{COP}, entropy production rates and exergy destruction rates for the finite heat capacity model in this study. According to Incropera and DeWitt (Incropera, F. P., DeWitt, D. P. 1996), the effectiveness of a heat exchanger is based upon the maximum possible heat transfer rate, q_{max} for the heat exchanger. In theory, the heat transfer rate can be determined by assuming a counter flow heat exchanger of infinite length. As such, one of the streams of this heat exchanger would be subjected to the maximum possible temperature difference, $(T_{h,i} - T_{c,i})$. Incropera and DeWitt illustrated this concept under two situations:

When the cold fluid would experience the larger temperature change, and because of the assumption that $L_{HX} \to \infty$, the cold fluid would be heated to the inlet temperature of the hot fluid until they reach equilibrium conditions $(T_{c,o} = T_{h,i})$. Thus:

$$C_c < C_h: q_{max} = C_c(T_{h,i} - T_{c,i}) \quad (30)$$

Likewise, for $C_h < C_c$ and $L_{HX} \to \infty$, the hot fluid would experience the larger temperature change and would be cooled down to the inlet temperature of the cold fluid $(T_{h,o} = T_{c,i})$. Then, for $C_h < C_c$:

$$q_{max} = C_h(T_{h,i} - T_{c,i}) \quad (31)$$

From the aforementioned results, a general expression is given by:

$$q_{max} = C_{min}(T_{h,i} - T_{c,i}) \quad (32)$$

Where C_{min} can be either C_c or C_h, based on whichever of the two is smaller. However, Eq. 32 is not equal to: $C_{max}(T_{h,i} - T_{c,i})$. Eq. 32 determines the maximum heat transfer that could possibly be delivered by the heat exchanger. The effectiveness can be represented by the ratio of the actual heat transfer for a heat exchanger to the maximum possible heat transfer rate:

$$eff = \frac{q}{q_{max}} \quad , 0 \leq eff \leq 1 \tag{33}$$

From equation 33 it follows that:

$$eff = \frac{C_h(T_{h,i} - T_{h,o})}{C_{min}(T_{h,i} - T_{c,i})} \tag{34}$$

In this study, it is assumed that $C_c = C_{min}$, and eq. 34 is reduced to:

$$eff = \frac{T_{h,i} - T_{h,o}}{T_{h,i} - T_{c,i}} \tag{35}$$

The *number of transfer units (NTU)* is a dimensionless parameter that is widely used for heat exchanger analysis and is defined as:

$$NTU = \frac{UA}{C_{min}} \qquad with \quad C_{min} = \dot{m} * C_p \tag{36}$$

Combining equations 35 and 36 yield the heat exchanger effectiveness relation:

$$eff = 1 - \exp(-NTU) \tag{37}$$

Equation 37 is used to determine the mass flow rates (which are assumed to remain constant throughout the cycle) across the heat exchangers interacting with the heat reservoirs and the absorption chiller's components as well as the working fluid temperatures $(T_1, T_2, T_3 and\ T_4)$ inside such components as shown in figure 4 (b). Once these values are known, the heat reservoir outlet temperatures are determined and then the heat transfer rates of the heat exchangers are calculated. Subsequently the COP, R_{COP}, entropy production rates

and exergy destruction rates for the finite heat capacity reservoir model are also determined. The heat transfer across the heat exchangers is explained in section 3.6.

3.6 Finite heat Capacity Model

As described in section 3.5, the effectiveness-NTU method is applied to the finite heat capacity reservoir model with the goal of determining the heat reservoir outlet temperatures. Such heat reservoir outlet temperatures are then used along with equations similar to eqs. 21-24 to determine the rates of heat transfer across each heat exchanger. The modified heat transfer rate equations applied to this model have been defined as

$$\dot{Q}_G = \dot{m}_G\left(h_{G,i} - h_{G,e}\right) \quad (38)$$

$$\dot{Q}_E = \dot{m}_E\left(h_{E,i} - h_{E,e}\right) \quad (39)$$

$$\dot{Q}_C = \dot{m}_C\left(h_{C,i} - h_{C,e}\right) \quad (40)$$

$$\dot{Q}_{\mathrm{A}} = \dot{m}_{\mathrm{A}}\left(h_{A,i} - h_{A,e}\right) \quad (41)$$

Where $\dot{m}_G, \dot{m}_E, \dot{m}_C \; and \; \dot{m}_A$ are the mass flowrates in the heat exchangers of the heat reservoirs interacting with the generator, evaporator, condenser and absorber respectively. $h_{G,i},\ h_{E,i}, h_{C,i} \; and \; h_{A,i}$ are the enthalpies at the inlet temperatures of the heat reservoirs interacting with the generator, evaporator, condenser and absorber respectively. The enthalpies with the subscripts "e" were calculated at the outlet/exit temperatures of the heat reservoirs. The reason behind using the heat transfer equations that depend on the enthalpy changes, is that since the inlet and outlet temperatures are known, EES software facilitates their calculations and thus the results obatined are more accurate. Once the heat transfers were determined, the COP, R_{COP}, entropy production rates and exergy destruction rates were calculated.

Since this model is more complex than the infinite heat capacity model, in the sense that mass flow rates and heat reservoir temperature changes are present, the entropy production and exergy destruction rates are calculated diffrerently than in the infinite heat capacity model case. The entropy production and exergy destruction rates are calculated by modifying equations 28 and 29 to:

$$\dot{\sigma} = -\Sigma_j \left(\frac{\dot{Q}_j}{T_k}\right) + \Sigma_j \dot{m}_j \left(s_{j,e} - s_{j,i}\right) \quad (42)$$

Where the subscript j represents the relation between heat reservoirs and absorption chiller's components $j = G, E, C, A$ and k represents the working fluid temperatures inside the absorption chiller's components $k = 1,2,3,4\ for\ G, E, C\ and\ A$. The terms $s_{j,e}\ and\ s_{j,i}$ represent the outlet/exit and inlet entropies at each of the heat exchangers.

The exergy destruction balance for this model is achieved by summing the individual exergy destruction rates. Such exergy destruction rates are obtained using the modified version of eq. 29 written as:

$$\dot{E}_{des} = \Sigma_j \left(1 - \frac{T_o}{T_k}\right) \dot{Q}_j + \Sigma_j\, \dot{m}_j (\boldsymbol{e}_{j,i} - \boldsymbol{e}_{j,o}) \quad (43)$$

Similar to eq. 42, j and k represent the same terms in eq. 43. The terms $\boldsymbol{e}_{j,i}\ and\ \boldsymbol{e}_{j,o}$ represent the inlet and outlet physical exergies for each heat exchanger. The physical exergies are calculated using eq. 4. (The analysis procedure for both model can be reviewed further in appendixes A and B.

3.7 New Themo-Ecological Approach

As described in section 2.7, thermo-ecological methods have been adopted and applied to absorption heat pumps and absorption refrigerators in order to determine the best operating configuration for a system while including the effect of the rate of entropy generation . A new performance criterion function, called the efficient power, which is defined as the multiplication of power by efficiency of the cycle was prosposed by Yilmaz (Yilmaz, T. et al 2006; Yilmaz, T. et al 2007). The proposed criterion considers not only the power output, but also the cycle efficiency, which in turn gives a compromise between power and efficiency. The efficient power criterion is defined as:

$$\dot{W}_{\eta} = \eta * \dot{W} \tag{44}$$

Where $\eta \; and \; \dot{W}$ are the efficiency and power output. The previous criterion, although it has only been mainly applied to heat engines in the past, is a good approach to determine the efficiency/power compromise and can be applied to absorption chillers as well. Because of that, this power criterion was implemented to both models described in sections 3.4 and 3.6. The original ecological criterion, presented in section 2.6 eq. (18) was also implemented to the models for comparison reasons. Both approaches eq. (18) and (44) take the form of:

$$ECOP1 = COP * R_{COP} \tag{45}$$

$$ECOP2 = R_{COP} - T_o * \dot{\sigma}_{gen} \tag{46}$$

Where ECOP1 is the efficient power criterion and thus the new thermo-ecological approach for the absortion chiller system. In equations (45) and (46) the terms $COP \; and \; R_{COP}$ are defined as:

$$COP = \frac{\dot{Q}_E - \dot{Q}_L}{\dot{Q}_G} \quad (47)$$

$$R_{COP} = \dot{Q}_E - \dot{Q}_L \quad (48)$$

Also, in the input paramater variation sections, the carnot COP for the system was calculated and compared to the COP "actual" of the system. The carnot COP applied to the system is described as:

$$COP_{car} = \left(\frac{T_{G1} - T_{CA}}{T_{G1}}\right)\left(\frac{T_{E1}}{(T_{CA} - T_{E1})}\right) \quad (49)$$

Where

$$T_{CA} = \frac{1 + \left(\frac{\dot{Q}_A}{\dot{Q}_C}\right)}{\left(\frac{1}{T_{C1}}\right) + \left(\frac{\dot{Q}_A}{\dot{Q}_C * T_{A1}}\right)} \quad (50)$$

The carnot COP was derived and defined previously (Hellmann, H. et al 2002)

4.0 Results and Discussion

4.1 Parametric Analysis: Infinite Heat Capacity Model

The next step of the analysis is the single variation for the input parameters (most important parameters) presented in table 3 for the infinite heat capacity model. As stated in section 3.3.1 the input parameters of highest importance are the inlet temperature of the heat reservoir interacting with the generator, the working fluid temperature inside the generator and the heat exchanger surface areas. The variations for the inlet temperature of the heat reservoir interacting with the generator as well as the working fluid temperature inside the

generator will be presented next, while the heat transfer surface areas and the heat transfer coefficients have been set to a specific fixed value.

4.1.1 Infinite Heat Capacity Model: Variation of inlet temperature T_{G1}

The inlet temperature of the heat reservoir interacting with the generator (T_{G1}) is varied from 400 K to 414 K, while keeping the working fluid temperature inside the generator (T_1) at a constant value of 390 K.

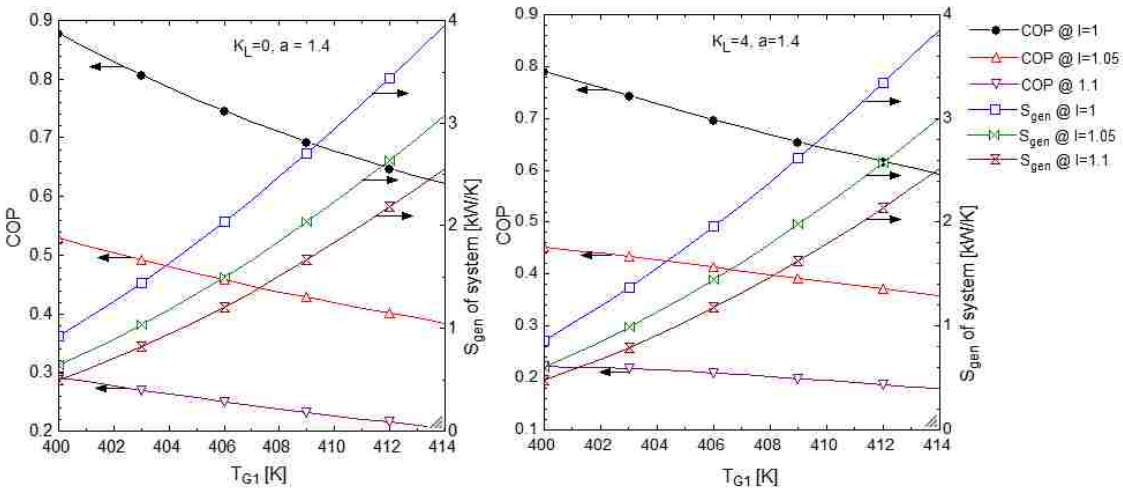

Figure 5: Infinite heat capacity model: COP & entropy generation vs. T_{G1}. Heat leak coefficient $K_L = 0\ \frac{kW}{K}$ (left), $K_L = 4\ \frac{kW}{K}$ (right).

The plots in figure 5 indicates that the COP of the system decreases while the entropy production of the system increases as the temperature T_{G1} is increased. Both COP and entropy production of the system decrease when the internal irreversibility factor "I" increases This indicates that the system's performance is highly sensitive to variations of "I". Once heat leakage is introduced to the system, the COP suffers a decrease in value while the rate of entropy generation suffers a small decrease as shown in figure 5 (right). In both cases

presented in figure 5, the COP and entropy generation decrease when the internal irreversibility factor "I" is increased.

The effects T_{G1} has on the exergy destruction of the system are presented in figure 6 for the cases where the heat leak coefficient is ($K_L = 0$) and ($K_L = 4$). In both cases, the exergy destruction increases with an increase of T_{G1}. The presence of a heat leak has a minimal effect on the exergy destruction as shown in figure 6.

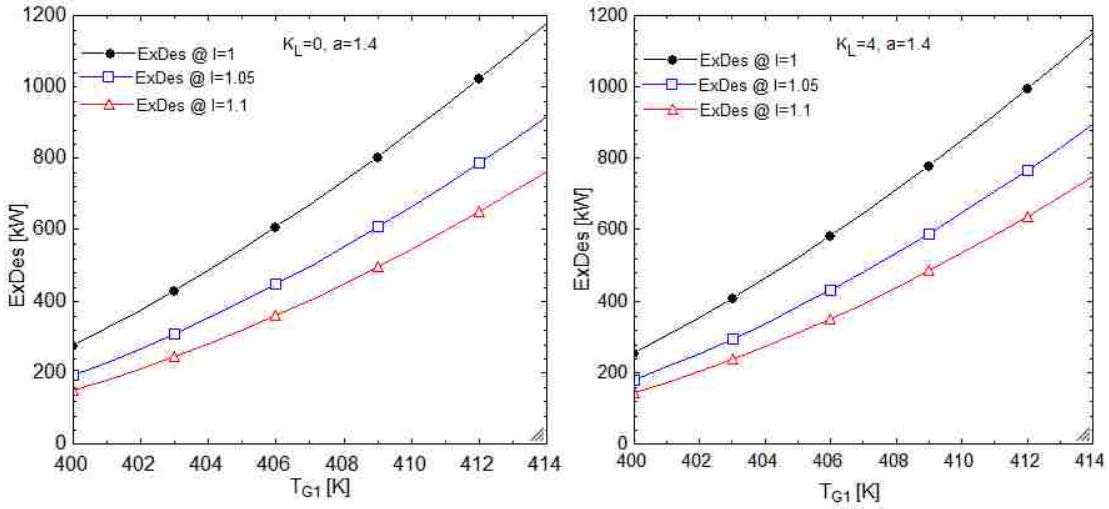

Figure 6: Infinite heat capacity model: Exergy destruction vs. T_{G1}. Heat leakage coefficient $K_L = 0\ \frac{kW}{K}$ (left), $K_L = 4\ \frac{kW}{K}$ (right).

Figure 7 displays the effects of T_{G1}on the COP, R_{COP} and ECOP1 [kW]. For both cases in figure 7, it can be seen that the COP decreases while R_{COP} and ECOP1 increases for an increase in T_{G1}, which agrees with the results presented in section 2. It can also be seen that the internal irreversibility factor "I" greatly impacts the performace of the system. Next, the ECOP1 and exergy destruction of the system will be compared.

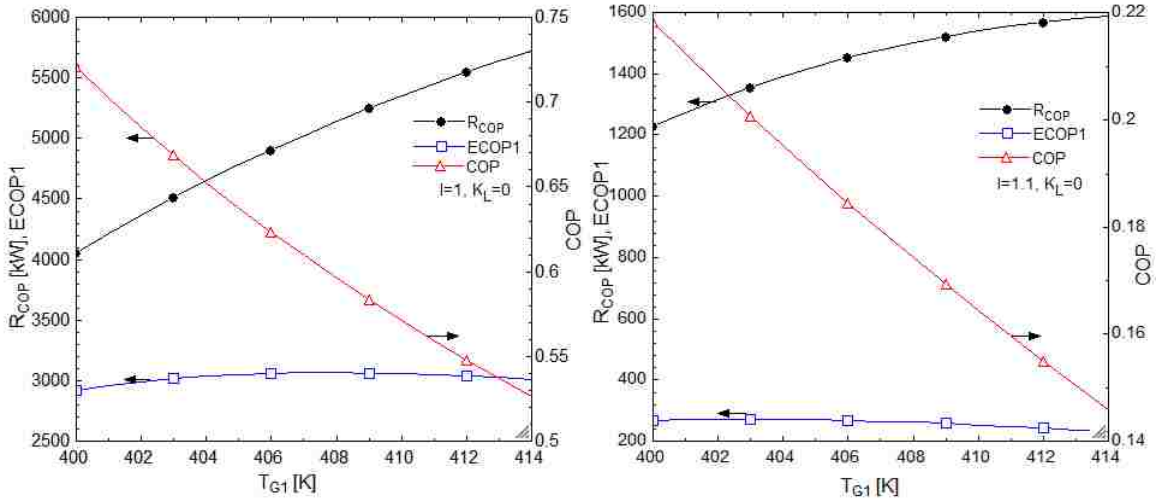

Figure 7: Infinite heat capacity model: $R_{COP}, ECOP1, COP\ vs. T_{G1}$. *With* $K_L = 0\ \frac{kW}{K}$ *@ I=1 (left) I=1.1 (right).*

In figure 8, it is shown that the exergy destruction increases while the value of ECOP1 increases reaching a maximum value at T_{G1}= 408 K and decreases after that point. As for the previous examples, the internal irreversibility affects the system's performance significantly.

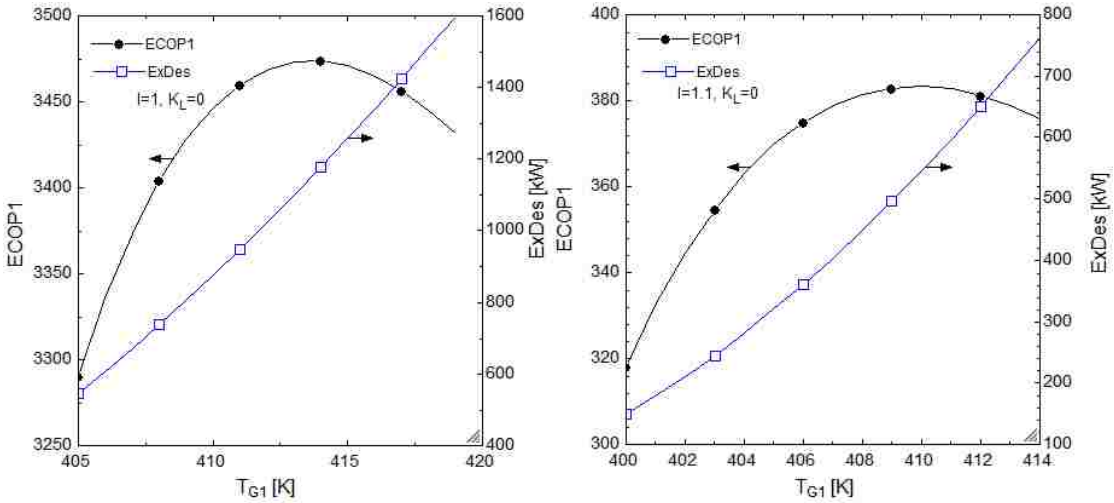

Figure 8: Infinite heat capacity model: ECOP1, Exergy destruction vs. T_{G1}. *I=1 (left). I=1.1 (right).*

As mentioned in section 3.7, the carnot COP was applied to both models. The plot for the COP_{car} and the infinite heat capacity model is presented next in figure 9.

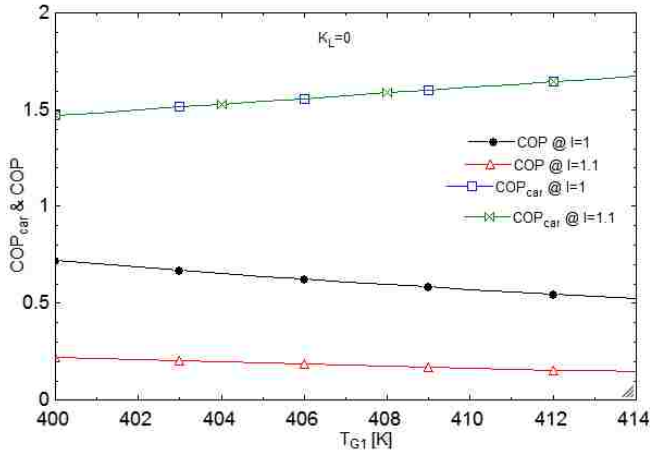

Figure 9: Infinite heat capacity model: COP_{carnot} & COP vs. T_{G1}.

In figure 9, it can be seen that the COP actual of the system is lower than the carnot COP. With the variations of T_{G1}, the COP decreases slowly while the carnot COP increases slightly. Again, the internal irreversibilities cause a significant decrease in COP while it has a minimal effect on COP_{car}.

4.1.2 Infinite Heat Capacity Model: Variation of the working fluid temperature T_1

The working fluid temperature inside the generator (T_1) is varied from 385 K to 399 K while keeping the inlet temperature (T_{G1}) of the heat reservoir which interacts with the gernerator fixed at 410 K. The first variation presented is that of the COP and entropy generation of the system (figure 10).

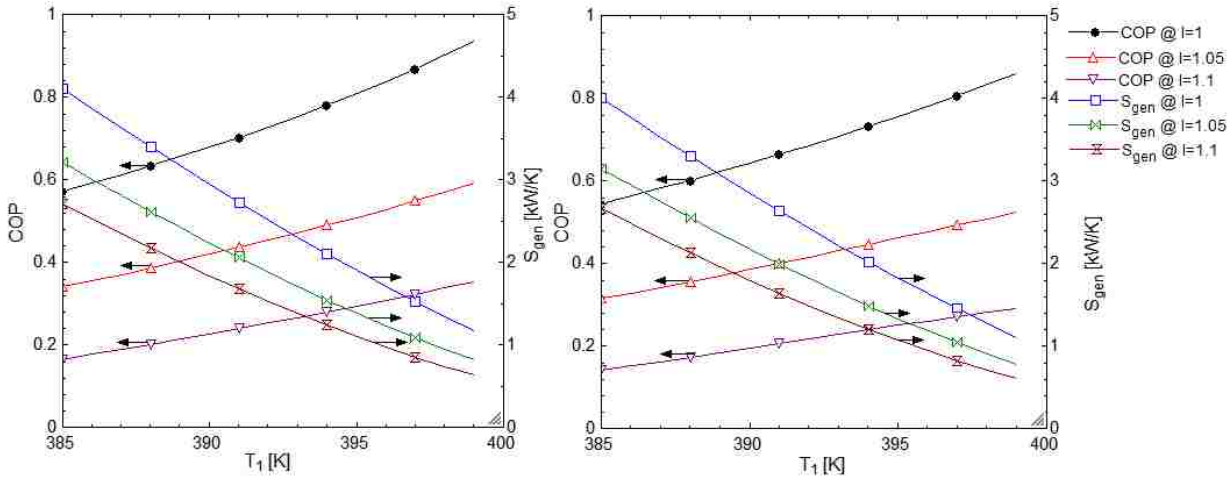

Figure 10: Infinite heat capacity model: COP & entropy generation vs T_1. At $K_L =$ $0\ \frac{kW}{K}\ (left) and\ K_L = 4\ \frac{kW}{K}\ (right)$.

As opposed to the results presented in figure 5, in figure 10 the COP increases while the entropy production of the system decreases with an increase of T_1. The COP and the entropy production of the system decrease when the internal irreversibility factor is increased. The heat leakage appears to have little effect on both the COP and entropy generation for the values used in this study.

The effects T_1 has over the exgergy destruction of the system are presented in figure 11. This figure shows that the exergy destructions of the system decrease with an increase of T_1. The exergy destructions are sensitive to an increase of the internal irreversibility factor but suffer little changes in the presence of a heat leakage. Also, when the heat reservoir inlet temperature T_{G1} is varied and the working fluid temperature T_1 is kept constant, opposite results are obatined. This means that the exergy destructions increase as T_{G1} increases.

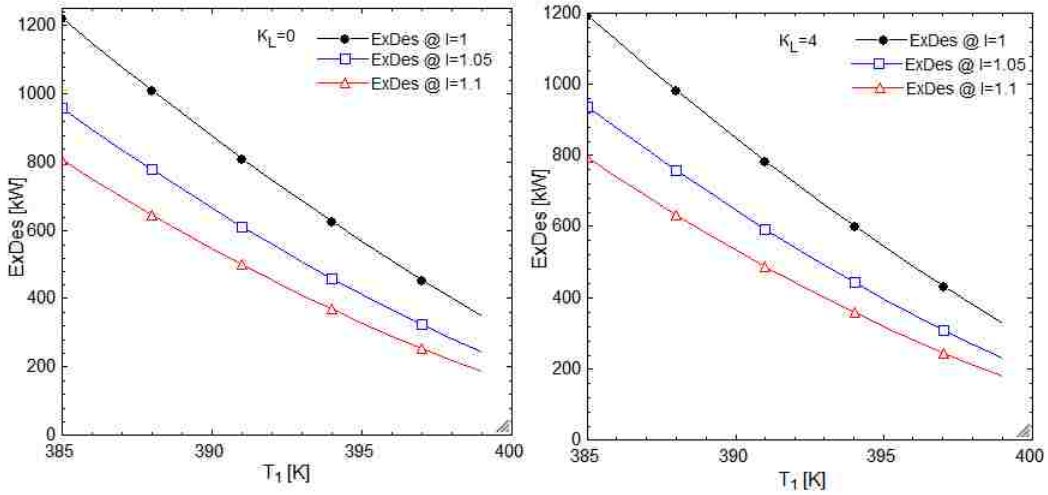

Figure 11: Infinite heat capacity model: Exergy destructions vs. T_1 *at* $K_L = 0\ \frac{kW}{K}\ (left) and\ K_L = 4\ \frac{kW}{K}\ (right)$.

The effects of the variations of T_1on the COP, R_{COP} and ECOP1 are presented in figure 12. In this figure, it is shown that the COP and the ECOP1 increase while R_{COP} decreases with an increase of T_1. It is also shown that changes internal irreversibility greatly impact the system's performance as both the COP and R_{COP} are significantly reduced.

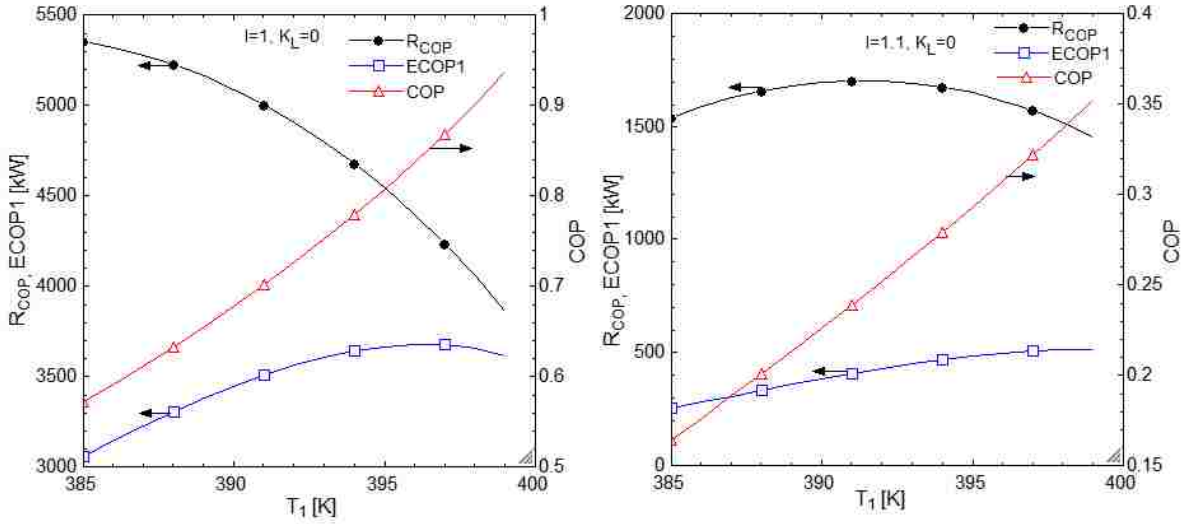

Figure 12: Infinite heat capacity model: $R_{COP}, ECOP1\ \&\ COP\ vs. T_1 at\ I = 1\ (left) and\ I = 1.1\ (right)$.

Similarly to the results shown in figure 8, figure 13 shows that the ECOP1 function increases reaching a maximum value at T_1=397 K, while the exergy destruction of the system decreases. Again, the internal irreversibilities have a significant impact on the system's performance.

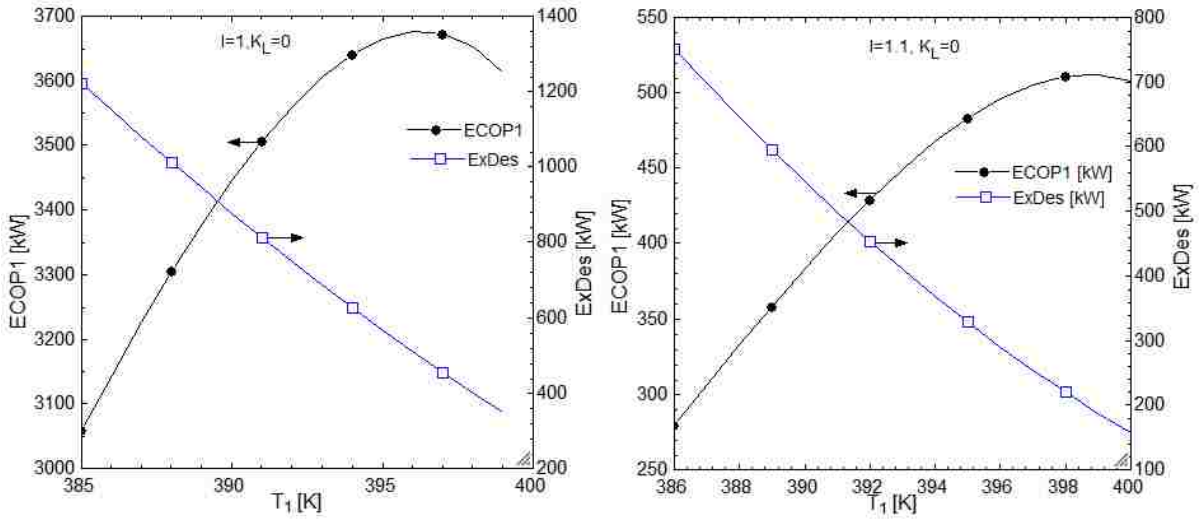

Figure 13: Infinite heat capacity model: ECOP1 & Exergy destruction vs. T_1 at $I = 1$ $(left)$ and $I = 1.1$ $(right)$.

Figure 14 shows that the COP is considerably lower than the COP_{car} and that it increases with an increase of T_1. As the internal irreversibility factor is increased, the COP decreases while the COP_{car} suffer small changes. The COP is decreased further when a heat leakage is introduced to the system.

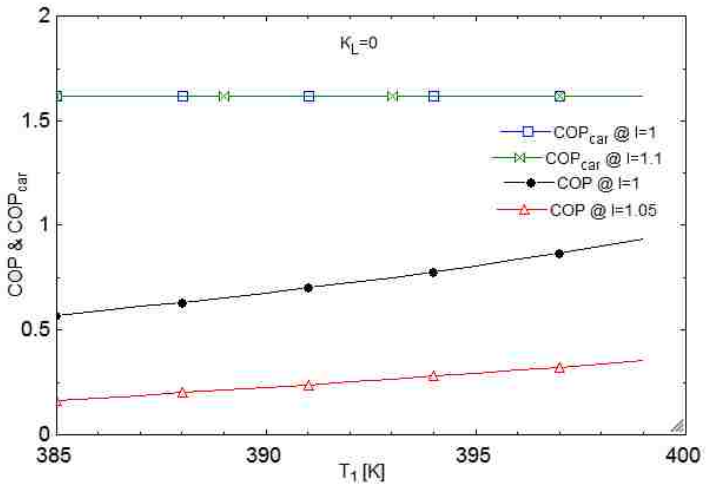

Figure 14: Infinite heat capacity model: COP carnot & COP vs $T_1 at\ K_L = 0\ \frac{kW}{K}$

The effects T_1has over the exergy destructions in each heat exchanger were also recorded and are shown in the subsequent graphs. As depicted in figure 15, the exgergy destruction in the heat exchangers decrease with at increase of T_1 (meaning that the COP of the system increasesas as shown in figure 14). Also, increasing the internal irreversibility factor value decreases the exergy destruction even further. This means that the internal exergy destructions have increase significantly. When a heat leakage is introduced to the system the exergy destrutions slightly increase, but the overall behavior is the same as shown in figure 11.

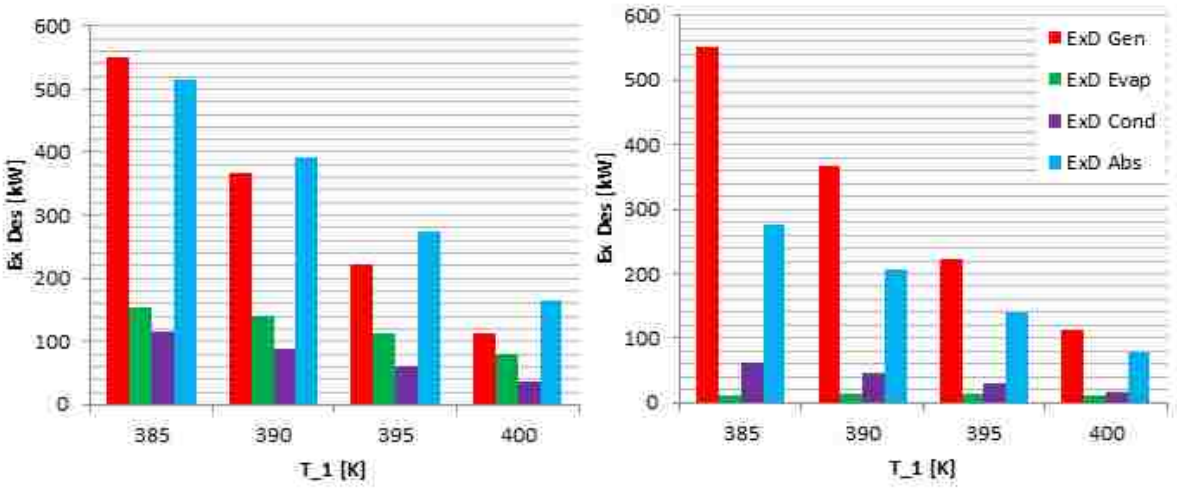

Figure 15: Infinite heat capacity model: Exergy destruction distribution in the heat exchangers interacting with the absorption chiller's internal components. Graphs recorder at $K_L = 0$, I=1 (left) and I=1.1 (right).

4.2 Parametric Analysis: Finite Heat Capacity Model

In this section of the analysis, the single variation for the input parameters for the finite heat capacity model will be performed. The input parameters to be varied in this section are the same as in section 4.1, and the variation ranges will be the same as well. The results for such variations are shown and explained next.

4.2.1 Finite Heat Capacity Model: Variation of inlet temperature T_{G1}

Similar to section 4.1.1, the inlet temperature of the heat reservoir interacting with the generator (T_{G1}) is varied from 400 K to 414 K, while keeping the working fluid temperature inside the generator (T_1) at a constant value of 390 K.

The results in figure 16 for the finite heat capacity model, show that this model follows a similar behavior as the infinite heat capacity model. For this case, the COP decreases while the entropy generation of the system increases with an increase in T_{G1}. Both

COP and entropy generation decrease in magnitude as the internal irreversibility factor is increased. Adding a heat leakage to the system causes the COP to decrease significantly, but has a smaller effect on the entropy generation.

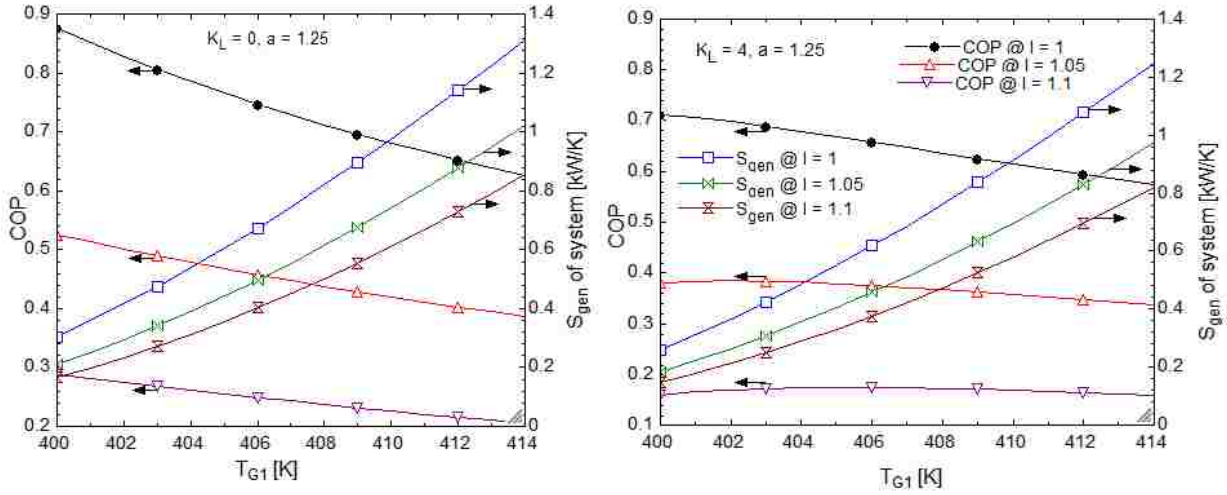

Figure 16: Finite heat capacity model: COP & entropy generation vs. T_{G1}. Heat leak coefficient $K_L = 0\ \frac{kW}{K}\ (left) and\ K_L = 4\ \frac{kW}{K}\ (right)$.

The exergy destruction of the system increases as T_{G1} increases, as shown in figure 17. Increasing the value of the internal irreversibility factor causes the exergy destruction of the system to decrease. Finally, the introduction of a heat leakage has little effect on the exergy destruction of the system as this suffers small changes.

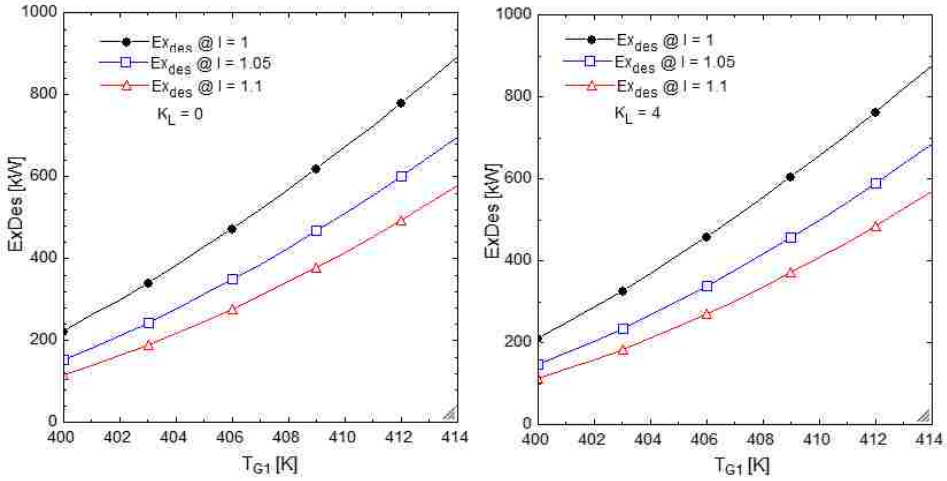

Figure 17: Finite heat capacity model: Exergy des truction vs. T_{G1}. No heat leakage $K_L = 0\frac{kW}{K}(left)$ and heat leakage $K_L = 4\frac{kW}{K}(right)$.

The effects that an increase in T_{G1}has over the R_{COP}, ECOP1 and COP are displayed in figure 18. For the cases shown, the R_{COP} increases, the COP decreases and the ECOP1 increase with an increase of T_{G1}. Again, the internal irreversibilities of the system have a significant impact on the system's performance as the COP and R_{COP} are greatly reduced when the factor "I" is increased.

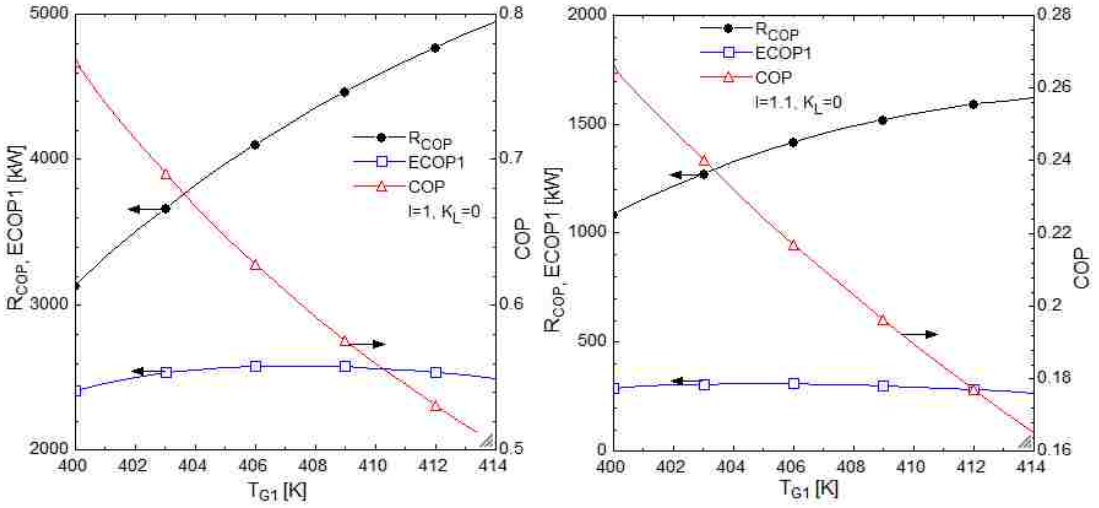

Figure 18: Finite heat capacity model: $R_{COP}, ECOP1, COP\ vs. T_{G1}$. With $K_L = 0\ \frac{kW}{W}$ at I=1 (left) I=1.1 (right).

Similar to the results shown in figure 8, figure 19 displays the behavior that ECOP1 follows with an increase of T_{G1}. ECOP1 increases reaching a maximum value at $T_{G1} = 407\ K$ and decreases after this point. It can also be seen that the internal irreversibility factor greatly impacts the value of ECOP1 but has little effect on the exergy destruction of the system which only shows a small decrease.

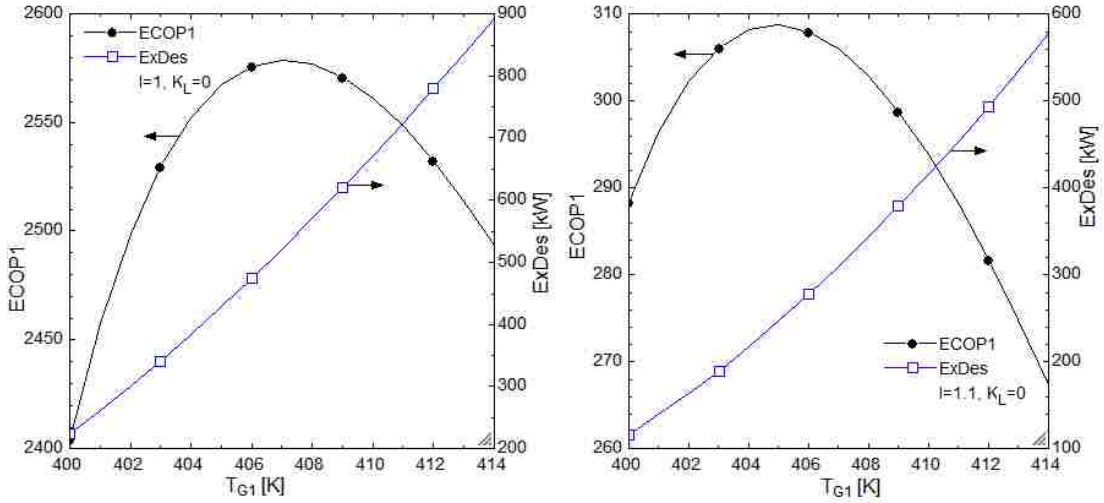

Figure 19: Finite heat capacity model: ECOP1, Exergy destruction vs T_{G1}. I=1 (left). I=1.1 (right).

The comparison between the COP and COP_{car} of the system is shown in figure 20. Here, the COP decreases and the COP_{car} increases as T_{G1} is increased. It is also shown that the COP is greatly reduced when the internal irreversibility factor is increased, which has been shown throughout this section.

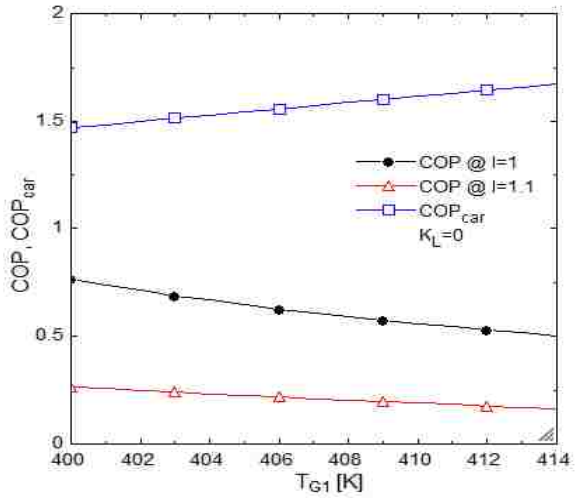

Figure 20: Finite heat capacity model: COP & COP_{car} $vs. T_{G1}$.

4.2.2 Finite Heat Capacity Model: Variation of the working fluid temperature T_1

In this section the same variations as in section 4.1.2 will be performed for the finite heat capacity model. The working fluid temperature inside the generator (T_1) is varied from 385 K to 399 K, while keeping the inlet temperature (T_{G1}) of the heat reservoir which interacts with the generator fixed at 410 K. The variation of the COP and entropy generation of the system, shown in figure 21.

The variations of T_1 cause the COP to increase while the entropy generation of the system decreases as shown in in figure 21. In this figure it is shown that, when increased, the internal irreversibility factor causes a decrease in COP and entropy generation. Heat leakage causes a decrease in both COP and entropy generation, having a larger effect on the COP for the values used in this study. The results shown in figure 21 are opposite to those in figure 16.

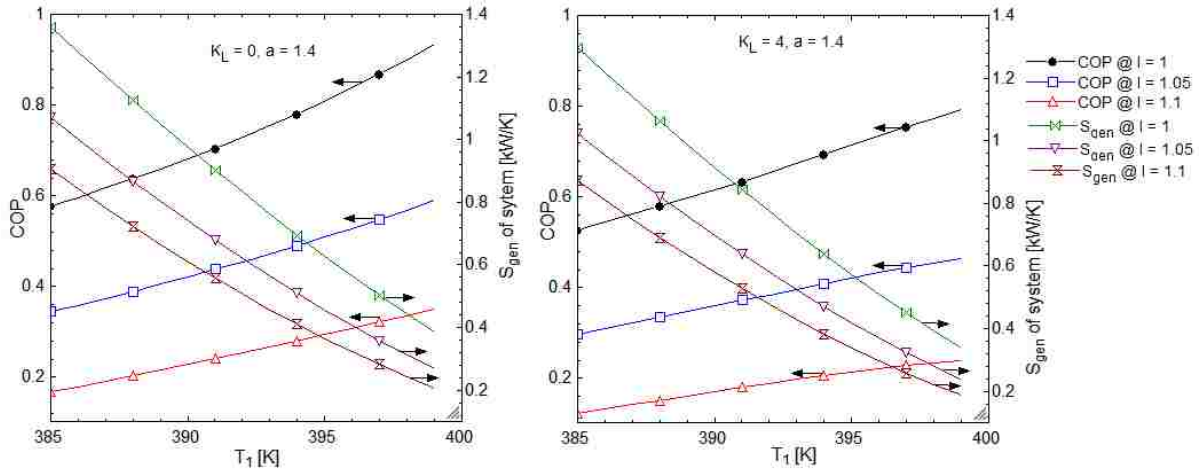

Figure 21: Finite heat capacity model: COP & entropy generation vs. T_1. At $K_L = 0\frac{kW}{K}(left) and\ K_L = 4\frac{kW}{K}(right)$.

Exergy destructions shown in figure 22 follow the behavior of the entropy generations of figure 21. The exergy destruction decreases when the internal irreversibility factor is increased. Heat leakages cause a small decrease on the values of the exergy destruction.

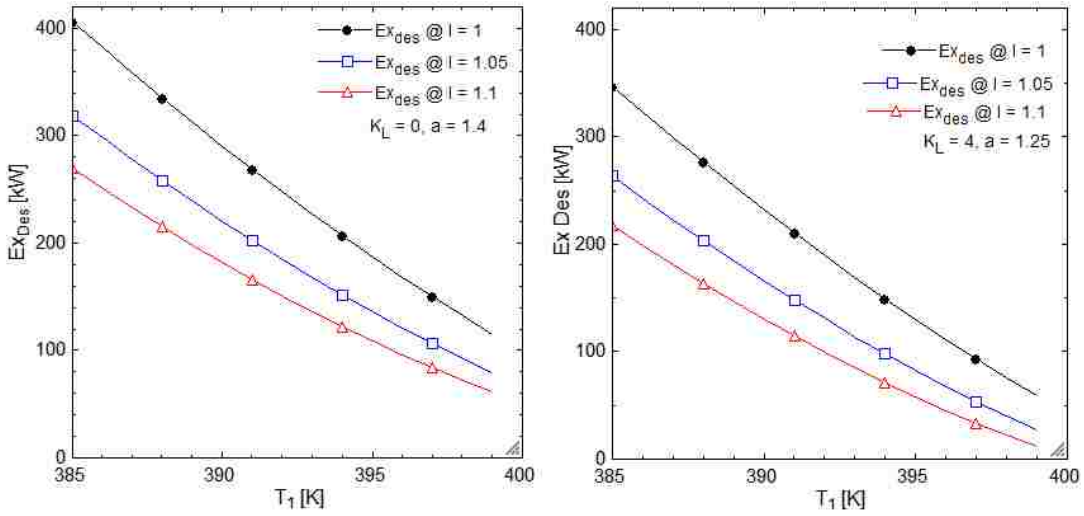

Figure 22: Finite heat capacity model: Exergy destructions vs. $T_1 at\ K_L = 0\frac{kW}{K}\ (left) and\ K_L = 4\ \frac{kW}{K}\ (right)$.

Opposite to the results of figure 18, in figure 23 the COP and ECOP1 increase while the R_{COP} decreases when $T_1$is increased. All values decrease significantly when the internal irreversibility factor is increased.

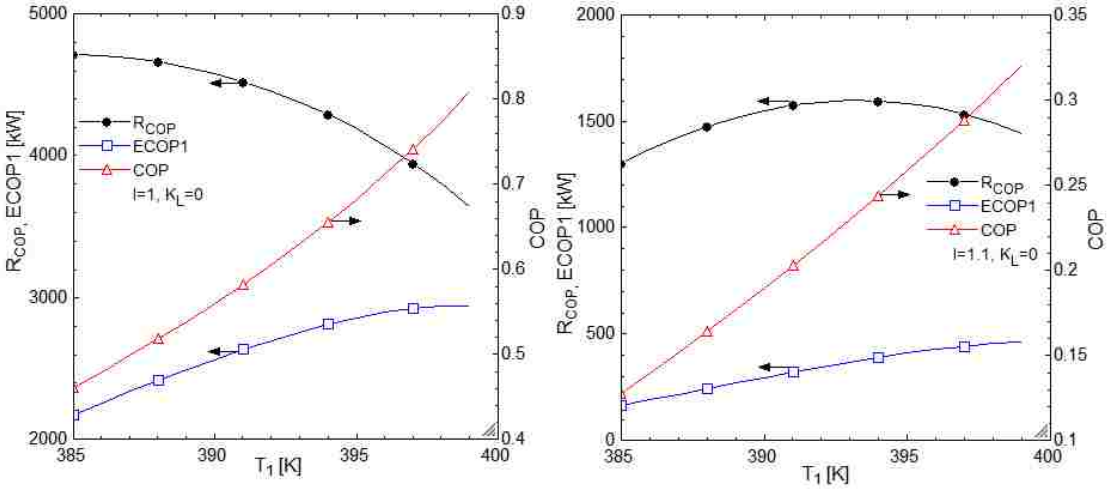

Figure 23: Finite heat capacity model: $R_{COP}, ECOP1$ & $COP\ vs. T_1 at\ I = 1\ (left) and\ I = 1.1\ (right)$.

Figure 24 shows that the ECOP1 function increases, reaching a maximum value at $T_1 = 397\ K$ while the exergy destruction decreases as T_1 increases. Also, heat leakages decrease the value of the ECOP1 function, but have a small impact on the exergy destructions. Increasing the internal irreversibility factor significantly reduces the value of the ECOP1 function, while the effet on the exergy destruction is small.

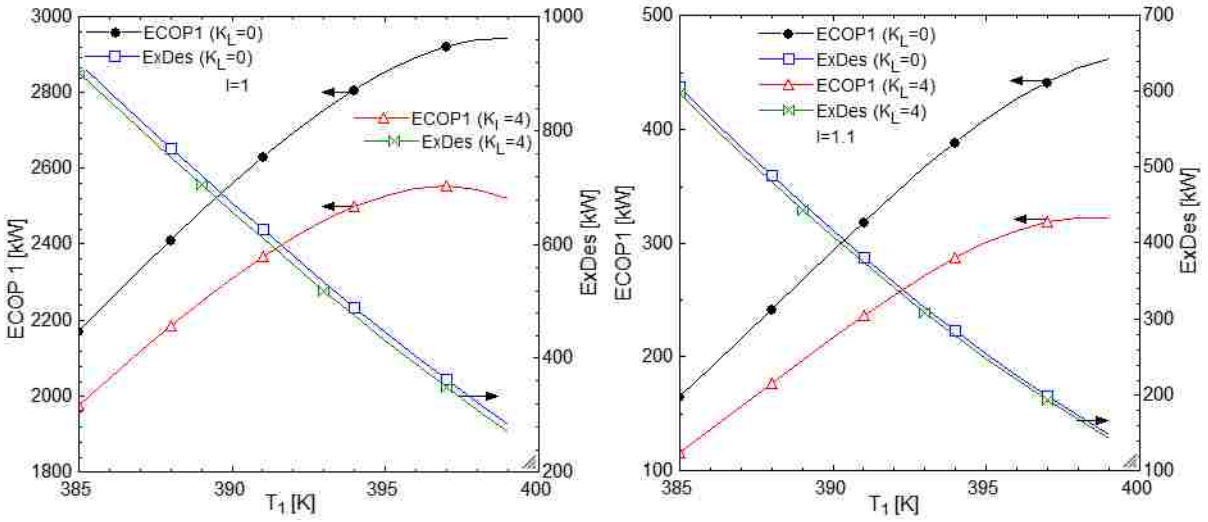

Figure 24: Finite heat capacity model: ECOP1 & Exergy destruction vs. T_1 at I=1 (left) and I=1.1 (right).

The COP of the system is compared to the COP_{car} in figure 25. It can be seen that the COP_{car} remains constant while increasing T_1. On the other hand, the COP "actual" of the system increases with the varitions of T_1. The COP is reduced when the internal irreversibility factor is increased.

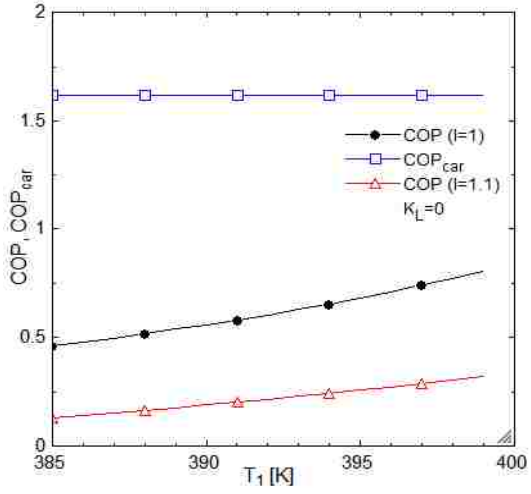

Figure 25. Finite heat capacity model: COP carnot & COP vs. $T_1 at\ K_L = 0$.

The exergy destructions due to the variations of T_1 in the heat exchangers interacting with the internal components of the system are presented in figure 26. As T_1 is increased, the exergy destructions decrease which indicates an increase of the system's COP. Incrementing the value of the internal irreversibility factor causes a decrease in the values of exergy destruction of the heat exchangers. The heat exchangers interacting with the evaporator and condenser undergo a larger decrease in exergy destruction. Heat leakages in the system cause a slight increase to the exergy destruction but are minimal when compared to the changes caused by an increase of the internal irreversibility factor. For the finite heat capacity model, if the working fluid temperature (T_1) is kept constant and variations to the inlet heat reservoir (T_{G1}) are performed, then the results obtained regarding the exergy destructions are the opposite to the results shown in figure 26 because the exergy differences (inlet to outlet) increase.

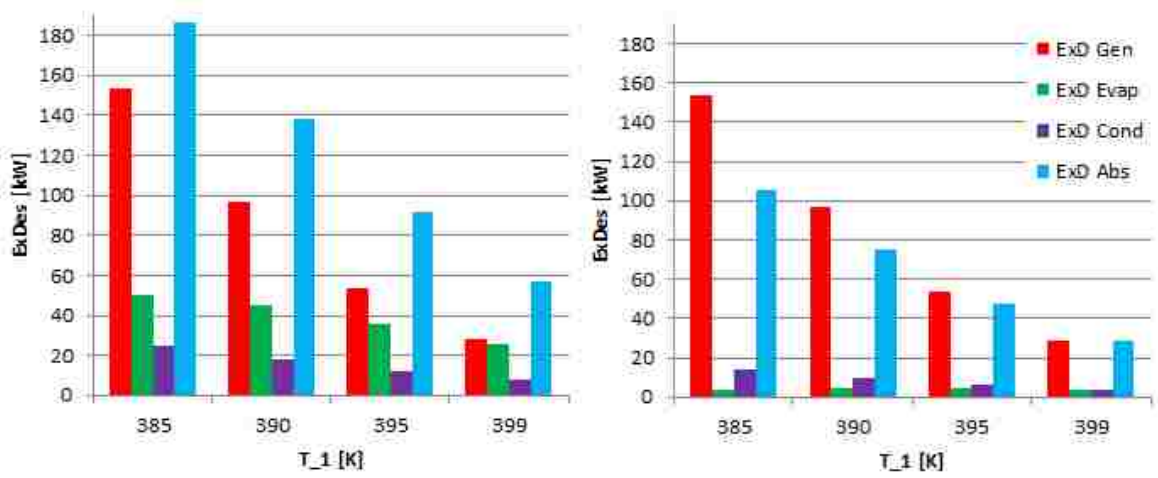

Figure 26: Finite heat capacity model: Exergy destruction distribution in the heat exchangers interacting with the absorption chiller's internal components. Graphs recorded at $K_L = 0$, I=1 (left) and I=1.1 (right).

Similar to the variations presented in (Chen, L. et al 2005), in this study, the effect of the internal irreversibility factor over the COP and R_{COP} was observed and is presented in figure 27. Here the internal irreversibility factor is changed from I=1 to I=1.1. With these variations, both the COP and R_{COP} suffer a reduction in values, which agrees with the results presented in (Chen, L. et al 2005).

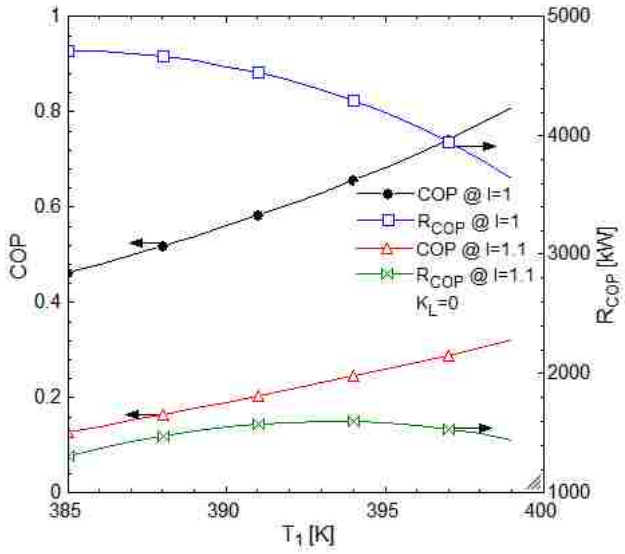

Figure 27: Infinite heat capacity model: COP, $R_{COP} vs. T_1$ for different values of the internal irreversibility factor I.

Another input parameter variation performed to the infinite heat capacity model was that of the heat leak coefficient. Mainly, the heat leak coefficeint was varied from 0 to 10 and the results of such variations are shown in figure 28. In figure 28, the COP vs R_{COP} plots follows a "loop" like shape, which is similar to the shape of figure 3 of section 2.5. For the cases shown in figure 28, it is shown that as the internal irreversibility factor is increased, both COP and R_{COP} are decreased. From these results, it can be concluded that the system

should be operated at the coditions that results in a high COP and cooling load value (the peak of the graphs in figure 28).

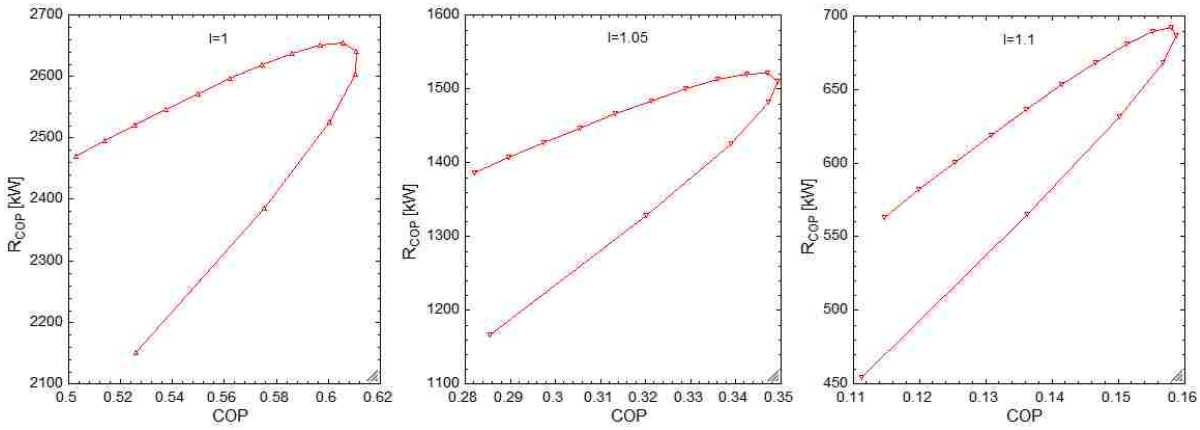

Figure 28: Infinite heat capacity model: COP vs Cooling load (R_{COP}), compromise for differerent I values.

5.0 Conclusion and Future Work

Application of the second-law analysis on a four temperature level absorption chiller was found to be very effective in determining the sytem's performances including the COP, R_{COP}, along with the exergy destructions across each heat exchanger that interacts between the different heat reservoirs and the internal components of the system. The analysis was carried out by taking into account the different irreversibilities that affect the overall performance of the system. A mathematical model that accurately represents the system was developed. In this model, with the help of the EES software, input parameter variations were performed in order to observe the effects these parameters had on the system's performance.

The effect of important system parameters on irreversibility distribution of selected basic components was analyzed. Also, a compromise between cooling rate and COP was observed for the absorption chiller used in the study. An ecological criterion previously used in analyzing power system was used to analyze a four-temperature absorption chiller model. In all calculations the conservation of energy and the balance of exergy were checked to make sure that the thermodynamic laws were not violated.

The infinite heat capacity model served as a base model to calculate energy and exergy balances, in order to ensure proper thermodynamic behavior. Once the proper energy and exergy calculations were carried out, input parameter variations demonstrated that, for the ranges selected, the system showed good performance and followed a proper behavior. The best results were obtained for the case of varying the working fluid temperature T_1 and holding the inlet heat reservoir temperature (T_{G1}) constant. As T_1 was increased, the system's COP increased signifying a higher efficiency and a reduced entropy generation, which in turn

meant a reduced exergy destruction in the system. It is important to recall that the working fluid temperature inside of the generator T_1 is of high importance, as the remaining internal temperatures dependend on it.

Since in actual applications it is very unlikely to have infinite heat capacity reservoirs, a more realistic approach was taken when the infinite heat capacity model was modified. This was done so that outlet heat reservoir temperatures could be calculated to change the base model to a finite heat capacity model. With this new model in mind, the application of the effectiveness-NTU method along with a second law approach helped determine the outlet heat reservoir temperatures which in turn were employed to determine a more realistic performance of the system.

For the modified finite heat capacity model, the input parameter variations revealed that the new model followed the same traits as the infinite heat capacity model in that the COP and exergy destrutions for both systems behaved similarly. In all cases, the infintite heat capacity model showed a higher COP and R_{COP} than the finite heat capacity model. At the same time however, the infinite heat capacity model showed a slightly higher entropy production and higher exergy destruction than the finite heat capacity model depending on which parameters were kept constant.

The application of a new performance criterion function along with the input parameter variation allowed us to determine the best operating conditions of the system for the variation ranges selected. This criterion had not been applied to as system similar to the one presented in this study. The efficiency power criterion function showed that the system reached a maximum value for all the variations performed. According to this criterion the

system should be operated at the highest value obtained, as it reflects the best compromise between the cooling power and efficiency of the system, which was the main goal of this study.

In both models it was shown that, when increased, the internal irrversibility factor "I" greatly diminishes the overall performance of the system. For this reason, this factor symbolizes a key topic to be explored further in future optmimization studies. Because of the nature of the models presented in this study, mainly that of the finite heat capacity reservoirs, the results found here are of high importance as these can be used in the optimization of systems of this nature. The methods employed here agree with and follow the thermodynamic laws which in turn gave accurate and realistic results that can serve as a baseline for future work related to absortion chillers working between four temperature levels of finite heat capacity.

Appendix A: Infinite heat capacity model ESS program

{Model 1: Infinite Heat Capacity Reservoirs}
{For this model, the heat transfers in the heat exchangers associated with the infinite heat capacity reservoirs and the internal components of an Absorption Chiller will be determined. This information will then be used to calculate the coefficient of performance (COP) and the cooling load of the system. Also, a thermo-ecological function will be applied to the system.}

{Step 1: Introduce parameters, that are to be varied or are fixed i.e. areas temperatures etc.}

{The surface areas of the heat exchangers are introduced next. These areas are parameters that will be varied in order to achieve the best operating conditions possible}

{A_G = 300}
{A_E = 350}
{A_C = 250}
{A_A = 430}

{The Heat Transfer Coefficients are introduced next}

U_G = 1.25 [kW/Km^2]
U_E = 2.5 [kW/Km^2]
U_C = 4.5 [kW/Km^2]
U_A = 1.25 [kW/Km^2]

{The heat reservoir temperatures and the ambient temperature are presented next. These temperatures are constant throughout the cycle of the system}

{T_G1= 413} {K}
T_E1 = 283 [K]
T_C1 = 333 [K]
T_A1 = 313 [K]
T_o = 298 [K]

{The parameter "a", presented below, represents the ratio of heat reject between the condenser and the absorber}

{a=1}

Q_dot_A = a * Q_dot_C

{Step 2: Calculate the heat transfers taking place between the heat reservoirs and the internal components of the Absorption Chiller}
{In order to calculate these heat transfers it is necessary to give an initial value (which can be varied) to the working fluid temperature in the generator. The reason for this is that this temperature is needed in order to calculate the remaining working fluid temperatures in the

condenser, absorber and evaporator as these are interdependent and needed to determine the numerical value for the heat transfers}

{T_1 = 363}
Q_dot_G = U_G * A_G * (T_G1 - T_1) *1 [kW]
Q_dot_E = U_E * A_E * (T_E1 - T_2) *1 [kW]
Q_dot_C = U_C * A_C * (T_3 - T_C1) *1 [kW]
Q_dot_A = U_A * A_A * (T_4 - T_A1) *1 [kW]

{Step 3: Introducing the heat leak and the system's internal irreversibility}
{Along with the heat transfers taking place between the heat reservoirs and internal components of the Absorption Chiller, there also exists a heat leak that affects the overall performance of the system. The heat leak (Q_dot_L) is presented next and the heat leak coefficient K_L dictates the magnitude of such heat leak}

{K_L = 3} {kW/K} {change to 1.5 later on}

Q_dot_L = K_L * (T_o - T_E1) *1 [kW]

{In order to simplify the complexity of the system and to be able to account for the irreversibilities taking place inside of the system, the parameter "I" is introduced. "I" represents the total internal irreversibilities of the system and is defined using the second law of thermodynamics as shown below}

{I = 1}
I = ((Q_dot_C / T_3) + (Q_dot_A / T_4)) / ((Q_dot_G / T_1) + (Q_dot_E / T_2))

{Step 4: Exergy destruction, entropy and energy balances will be calculated. This is done in order to confirm that the mathematical model behaves correctly and that it follows an accurate thermodynamic behavior}

{The irreversibitiles between the heat reservoirs and the internal components are calculated as:}

sigma_dot_G = - (Q_dot_G * ((1/T_G1) - (1/T_1))) * 1[kW/K]
sigma_dot_E = - (Q_dot_E * ((1/T_E1) - (1/T_2))) * 1 [kW/K]
sigma_dot_C = - (Q_dot_C * ((1/T_3) - (1/T_C1))) * 1 [kW/K]
sigma_dot_A = - (Q_dot_A * ((1/T_4) - (1/T_A1))) * 1 [kW/K]

{The total entropy of the system and the entropy balance are shown below}

sigma_total = (sigma_dot_G + sigma_dot_E + sigma_dot_C + sigma_dot_A + sig_L_E) * 1 [kW/K]
entropy_bal = sigma_total * T_o * 1 [kW]

{The exergy destructions between the heat reservoirs and the internal components are calculated as:}

E_D_G = Q_dot_G * (T_o * ((1/T_1) - (1/ T_G1))) * 1 [kW]
E_D_E = Q_dot_E * (T_o * ((1/T_2) - (1/T_E1))) * 1 [kW]
E_D_C = Q_dot_C * (T_o * ((1/T_C1) - (1/T_3)))   * 1 [kW]
E_D_A = Q_dot_A * (T_o * ((1/T_A1) - (1/T_4)))   * 1 [kW]

{The Exergy destruction balance for the system is:}

Exergy_destruction_sys = E_D_G + E_D_E + E_D_C + E_D_A + ex_L_E {kW}

{The energy balance of the system is presented next. This expression contains the heat leakage}

Q_dot_G + Q_dot_E - Q_dot_C - Q_dot_A - Q_dot_L = 0 {kW}
Energy_bal = Q_dot_G + Q_dot_E - Q_dot_A - Q_dot_C - Q_dot_L {kW}

{Calculating the irreversibilities due to the heat leak. These will be added to the total entropy of the system and the exergy destruction of the system}

sig_L_E = - Q_dot_L * ((1 / T_o) - (1 / T_E1)) {kW/K}

ex_L_E = - Q_dot_L * (1 - (T_o / T_E1)) {kW}

{Step 5: COP and cooling capacity of the system are calculated next}

{The Coefficient of performance is calculated following the classical definition shown next}

COP = (Q_dot_E - Q_dot_L) / Q_dot_G

{From the classical definition, the COP Carnot can be calculated employing the temperatures of the heat reservoirs only, or with the combination of heat transfer and the temperature of the heat reservoirs. Both methods are presented next}

COP_carnot = (T_E1 / (T_C1 - T_E1)) * ((T_G1 - T_C1) / T_G1)

T_CA = (1 + (Q_dot_A / Q_dot_C)) / ((1 / T_C1) + (Q_dot_A / (Q_dot_C * T_A1)))

COP_car = ((T_G1 - T_CA) / T_G1) * (T_E1 / (T_CA - T_E1))

{Next, the cooling capacity of the system is calculated. This value depends on the heat transfer that takes place in the evaporator and is affected by the heat leakage}

R_COP = Q_dot_E - Q_dot_L

{Next the ecological functions will be applied to the system}

ECOP_1 = R_COP * COP
ECOP_2 = R_COP - T_o * sigma_total

Appendix B: Finite heat capacity model EES program

{Model 2: "Finite Heat Capacity Reservoirs"}
{For this model, the heat reservoirs that interact with the absorption chiller components have a finite heat capacity meaning that the temperature of the heat reservoirs is not constant throughout the cycle but these either increase or decrease depending on the component they interact with. The working fluid temperature in each of the internal components of the Absorption Chiller is assumed to be constant but interdependent. Since the working fluid temperatures are interdependent, these temperatures will be calculated using the first and second laws of thermodynamics. Also, the internal temperatures will be employed to calculate the exiting temperatures of the heat reservoirs by means of the effectiveness-NTU method.}

{Step 1: Introduce parameters, that are to be varied or are fixed i.e. areas temperatures etc.}
{The surface areas of the heat exchangers are introduced next. These areas are parameters that will be varied in order to achieve the best operating conditions possible.}

A_G = 300 [m^2]
A_E = 300 [m^2]
A_C = 300 [m^2]
A_A = 300 [m^2]

U_G = 2.5 [kW/Km^2]
U_E = 2.5 [kW/Km^2]
U_C = 2.5 [kW/Km^2]
U_A = 2.5 [kW/Km^2]

{The heat leak coefficiecnt is shown below. The specific heat of air will be calculated using EES}

{K_L = 0 } {kW/K}
C_p = SpecHeat(Air_ha,T=T_o,P=P) * 1 [kJ/kg*K]

{The inlet heat reservoir temperatures are introduced next. With the exception of the temperature of the heat reservoir interacting with the generator, the other inlet temperatures are assumed to be constant. Also, an initial value is given to the working fluid temperature in the generator (this temperature will also be varied in order to observe the effects it has on the system's overall performance).}

{T_1 = 390} {K}
{T_G1= 413} {K}
T_E1 = 283 [K]
T_C1 = 333 [K]
T_A1 = 313 [K]
T_o = 298 [K]
P = 0.101325 [MPa]

{Step 2: Preliminary heat transfer calculation}
{This heat transfer calculations are intended to determine the value of the working fluid temperatures inside each of the components of the Absorption Chiller. Once these temperatures are know, they will be used to calculate the outlet temperatures of the heat reservoirs.}

Q_G = m_dot_G * C_p * (T_G1 - T_1) * 1 [kW]
Q_E = m_dot_E * C_p * (T_E1 - T_2) * 1 [kW]
Q_C = m_dot_C * C_p * (T_3 - T_C1) * 1[kW]
Q_A = m_dot_A * C_p * (T_4 - T_A1) * 1 [kW]

{The parameter "a" represents the heat reject ratio between the absorber and condenser}

{a = 1.25}
Q_dot_A = a * Q_dot_C

{Step 3: Application of the effectiveness-NTU method}
{The effectiveness-NTU method is applied to calculate the heat reservoir outlet temperatures and the corresponding mass flow rates. The mass flow rates are assumed to be constant through each heat exchanger}

epsilon = 0.75

epsilon = (T_G1 - T_G2) / (T_G1 - T_1)
epsilon = (T_E1 - T_E2) / (T_E1 - T_2)
epsilon = (T_C1 - T_C2) / (T_C1 - T_3)
epsilon = (T_A1 - T_A2) / (T_A1 - T_4)

m_dot_G = - (U_G * A_G) / (ln (1 - epsilon) * C_p) {kg/s}
m_dot_E = - (U_E * A_E) / (ln (1 - epsilon) * C_p) {kg/s}
m_dot_C = - (U_C * A_C) / (ln (1 - epsilon) * C_p) {kg/s}
m_dot_A = - (U_A * A_A) / (ln (1 - epsilon) * C_p) {kg/s}

{Now, the enthalpies, entropies, exergies, and heat transfers will be calculated using the reservoir's inlet and outlet temperatures}

{Step 4: Enthalpy calculations at intet and outlet temperatures}

h_G_in = enthalpy(Air_ha,T=T_G1,P=P)
h_E_in = enthalpy(Air_ha,T=T_E1,P=P)
h_C_in = enthalpy(Air_ha,T=T_C1,P=P)
h_A_in = enthalpy(Air_ha,T=T_A1,P=P)

h_G_out = enthalpy(Air_ha,T=T_G2,P=P)

```
h_E_out = enthalpy(Air_ha,T=T_E2,P=P)
h_C_out = enthalpy(Air_ha,T=T_C2,P=P)
h_A_out = enthalpy(Air_ha,T=T_A2,P=P)

h_o = enthalpy(Air_ha,T=T_o,P=P)

{Step 5: Entropy calculations at the inlet and outlet temperatures}

s_G_in = Entropy(Air_ha,T=T_G1,P=P)
s_E_in = Entropy(Air_ha, T=T_E1,P=P)
s_C_in = entropy(Air_ha, T=T_C1,P=P)
s_A_in = Entropy(Air_ha, T=T_A1,P=P)

s_G_out = Entropy(Air_ha,T=T_G2,P=P)
s_E_out = Entropy(Air_ha,T=T_E2,P=P)
s_C_out = Entropy(Air_ha,T=T_C2,P=P)
s_A_out = Entropy(Air_ha,T=T_A2,P=P)

s_o = Entropy(Air_ha,T=T_o,P=P)

{Step 6: Calculate the heat transfers using previously defined parameters (mass flow rates, enthalpies and temperatures)}

Q_dot_G = m_dot_G * ( h_G_in - h_G_out )
Q_dot_E = m_dot_E  * ( h_E_in - h_E_out )
Q_dot_C = m_dot_C * ( h_C_out - h_C_in )
Q_dot_A = m_dot_A * ( h_A_out - h_A_in )

{Step 7: Define the heat leaks in the system}

Q_dot_L =  K_L * (  T_o - T_E1 )

{Step 8: With the heat transfers at hand, the next step consists of constraining these heat transfers using the 1st and 2nd laws of thermodynamics}

{The first law of thermodynamics}

Q_dot_G + Q_dot_E - Q_dot_C - Q_dot_A  - Q_dot_L = 0

{The second law of thermodynamics}
{I =1}

I  = ( ( Q_dot_C / T_3 ) + ( Q_dot_A / T_4 )) /  ( ( Q_dot_G / T_1 ) + ( Q_dot_E / T_2 ) )


{Step 9: Rates of entropy production will be calculated next}
```

sigma_G = Q_dot_G * (1 / T_1) + m_dot_G * (s_G_out - s_G_in)
sigma_E = Q_dot_E * (1 / T_2) + m_dot_E * (s_E_out - s_E_in)
sigma_C = - Q_dot_C * (1 / T_3) + m_dot_C * (s_C_out - s_C_in)
sigma_A = - Q_dot_A * (1 / T_4) + m_dot_A * (s_A_out - s_A_in)

sigma_production_system = sigma_G + sigma_E + sigma_C + sigma_A + sig_L_E

Entropy_bal = sigma_production_system * T_o

{Step 10: Exergies at the inlet and outlets of the reservoirs will be calculated}

e_G_in = (h_G_in - h_o) - T_o * (s_G_in - s_o)
e_E_in = (h_E_in - h_o) - T_o * (s_E_in - s_o)
e_C_in = (h_C_in - h_o) - T_o * (s_C_in - s_o)
e_A_in = (h_A_in - h_o) - T_o * (s_A_in - s_o)

e_G_out = (h_G_out - h_o) - T_o * (s_G_out - s_o)
e_E_out = (h_E_out - h_o) - T_o * (s_E_out - s_o)
e_C_out = (h_C_out - h_o) - T_o * (s_C_out - s_o)
e_A_out = (h_A_out - h_o) - T_o * (s_A_out - s_o)

{Step 11: Rates of exergy destruction will be calculated and the exergy balance will be determined}

E_dot_G = - Q_dot_G * (1 - (T_o / T_1)) + m_dot_G * (e_G_in - e_G_out)
E_dot_E = - Q_dot_E * (1 - (T_o / T_2)) + m_dot_E * (e_E_in - e_E_out)
E_dot_C = Q_dot_C * (1 - (T_o / T_3)) + m_dot_C * (e_C_in - e_C_out)
E_dot_A = Q_dot_A * (1 - (T_o / T_4)) + m_dot_A * (e_A_in - e_A_out)

Exergy_destruction_system = E_dot_G + E_dot_E + E_dot_C + E_dot_A + ex_L_E

{Step 12 : Next, the energy balance will be determined}

Energy_bal = Q_dot_G + Q_dot_E - Q_dot_A - Q_dot_C - Q_dot_L

{Step 13: calculate the rates of entropy production due to the heat leaks}

sig_L_E = - Q_dot_L * ((1 / T_o) - (1 / T_2))

sig_E_loss = sig_L_E * T_o

{Step 14: Calculate the rate of exergy destruction due to the heat leaks}

ex_L_E = - Q_dot_L * (1 - (T_o / T_2))

{The diff (below) represents the difference between the exergy destruction balance and the product between the rate of entropy production and the ambient temperature. The result of such difference should equal 0 }

diff = Exergy_destruction_system - Entropy_bal

{Step 15: Determining the COP and Cooling load of the system (R_COP)}

{The COP of the system which from classical definitions depends on the heat transfer between the heat reservoirs and the generator and evaporator is the following}
{The COP is also affected by the heat leakage}

COP = (Q_dot_E - Q_dot_L) / Q_dot_G
R_COP = Q_dot_E - Q_dot_L

{The Carnot COP will also be calculated and used as a base line to compare it vs the system's COP}

COP_carnot = (T_E1 / (T_C1 - T_E1)) * ((T_G1 - T_C1) / T_G1)

T_CA = (1 + (Q_dot_A / Q_dot_C)) / ((1 / T_C1) + (Q_dot_A / (Q_dot_C * T_A1)))
COP_car = ((T_G1 - T_CA) / T_G1) * (T_E1 / (T_CA - T_E1))

{Next step: Calculate the different ECOPs of the system using the available formulas}

ECOP_1 = R_COP * COP
ECOP_2 = R_COP - T_o * sigma_production_system

References

1. “Manual for single-stage Li-Br water absorption chiller.” *Development Division, Ebara Corp., Fujisawa, Japan, 1995.*
2. Abdulateef, J. M., Alghoul, M. A., Sirwan, R., Zaharim, A., Sopian, K.; “Second law thermodynamic analysis of a solar single-stage absorption refrigeration system.” *Models and Methods in Applied Sciences, (2012) 163-168.*
3. Abrahamsson, K., and Å. Jernqvist. "Carnot comparison of multi-temperature level absorption heat cycles." *International journal of refrigeration* 16.4 (1993): 240-246.
4. Acikkalp, Emin. "Modified thermo-ecological optimization for refrigeration systems and an application for irreversible four-temperature-level absorption refrigerator." *International Journal of Energy and Environmental Engineering* 4.1 (2013): 1-9.
5. Andresen, Bjarne, Peter Salamon, and R. Stephen Berry. "Thermodynamics in finite time." *Phys. Today* 37.9 (1984): 62-70.
6. Angulo-Brown, F. "An ecological optimization criterion for finite-time heat engines." *Journal of Applied Physics* 69.11 (1991): 7465-7469.
7. Bejan, A., J. V. C. Vargas, and M. Sokolov. "Optimal allocation of a heat-exchanger inventory in heat driven refrigerators." *International journal of heat and mass transfer* 38.16 (1995): 2997-3004.
8. Bejan, Adrian, and Michael J. Moran. *Thermal design and optimization*. John Wiley & Sons, 1996.
9. Bhardwaj, P. K., S. C. Kaushik, and Sanjeev Jain. "Finite time optimization of an endoreversible and irreversible vapour absorption refrigeration system."*Energy conversion and management* 44.7 (2003): 1131-1144.
10. Chen, Jincan, and Bjarne Andresen. "Optimal analysis of primary performance parameters for an endoreversible absorption heat pump." *Heat Recovery Systems and CHP* 15.8 (1995): 723-731.
11. Chen, Jincan, and Jan A. Schouten. "Optimum performance characteristics of an irreversible absorption refrigeration system." *Energy conversion and management* 39.10 (1998): 999-1007.
12. Chen, Jincan. "Optimal performance analysis of irreversible cycles used as heat pumps and refrigerators." *Journal of Physics D: Applied Physics* 30.4 (1997): 582.
13. Chen, Jincan. "The equivalent cycle system of an endoreversible absorption refrigerator and its general performance characteristics." *Energy* 20.10 (1995): 995-1003.
14. Chen, Jincan. "The optimum performance characteristics of a four-temperature-level irreversible absorption refrigerator at maximum specific cooling load."*Journal of Physics D: Applied Physics* 32.23 (1999): 3085.

15. Chen, L., F. Sun, and C. Wu. "The influence of heat-transfer law on the endo-reversible Carnot refrigerator." *Journal of the Institute of Energy* 69.479 (1996): 96-100.
16. Chen, Lingen, et al. "Irreversible four-temperature-level absorption refrigerator."*Solar energy* 80.3 (2006): 347-360.
17. Chen, Lingen, Fengrui Sun, and Chih Wu. "Effect of heat transfer law on the performance of a generalized irreversible Carnot refrigerator." *Journal of Non-Equilibrium Thermodynamics* 26.3 (2001): 291-304.
18. Chua, H. T., et al. "Entropy production analysis and experimental confirmation of absorption systems." *International journal of refrigeration* 20.3 (1997): 179-190.
19. Chua, H. Tong, et al. "Thermodynamic modeling and experimental evidence for the optimization and maximum-efficiency operation of absorption chillers." *ECOS* 96 (1996): 157-166.
20. Curzon, F. L., and B. Ahlborn. "Efficiency of a Carnot engine at maximum power output." *American Journal of Physics* 43.1 (1975): 22-24.
21. Davis, Gregory W., and Chih Wu. "Finite time analysis of a geothermal heat engine driven air conditioning system." *Energy conversion and management*38.3 (1997): 263-268.
22. Garland, R. W., and P. W. Adcock. *Refrigeration in a World without CFCs*. No. CONF-960730--5. Oak Ridge National Lab., TN (United States), 1996.
23. Gordon, Jeffrey M., and K. Choon Ng.; Cool thermodynamics. *Cambridge Int. Science Publishers, Cambridge* (2000).
24. Goth, Y., Feidt, M. “Optimum COP for endoreversible heat pump or refrigerating machine.” *C.R. Acad. Aci. Paris 303, (1986) 19-24.*
25. Hellmann, Hans-Martin. "Carnot-COP for sorption heat pumps working between four temperature levels." *International journal of refrigeration* 25.1 (2002): 66-74.
26. Herold, Keith E., Reinhard Radermacher, and Sanford A. Klein. *Absorption chillers and heat pumps*. CRC press, 1996.
27. Huang, Yuewu, Dexing Sun, and Yanming Kang. "Performance optimization for an irreversible four-temperature-level absorption heat pump." *International Journal of Thermal Sciences* 47.4 (2008): 479-485.
28. Incropera, F. P., DeWitt, D. P.; Introduction to heat transfer third edition. *John Wiley & Sons, Inc. 1996 pp. 561-563.*
29. Kaushik, S. C., C. S. Tomar, and S. Chandra. "Coefficient of performance of an ideal absorption cycle." *Applied Energy* 14.2 (1983): 115-121.
30. Klein, S. A. Engineering Equation Solver (EES) for Microsoft windows operating systems. Commercial and professional version. F: Chart software, Madison, Wisconsin, 2006.

31. Medrano, M., H. Gebreslassie, B., Boer, D. “Exergy analysis of multi-effect water-LiBr Absorption Systems from Half to Triple Effect.” *International Journal of Renewable Energy, vol. 35, (2010), pp 1773-1782.*
32. Ng, K. C., et al. "Thermodynamic modeling of absorption chiller and comparison with experiments." *Heat transfer engineering* 20.2 (1999): 42-51.
33. PanahiZadeh, Farshad, and Navid Bozorgan. "The energy and exergy analysis of single effect absorption chiller." *International Journal of Advanced Design and Manufacturing Technology* 4.4 (2011): 19-26.
34. Tang, T., Villareal, L., Green, J.; Absorption chillers: Southern California gas company new building institute advanced design guideline series. *New Building Institute, 1998.*
35. Tozer, Robert M., and Ron W. James. "Fundamental thermodynamics of ideal absorption cycles." *International journal of refrigeration* 20.2 (1997): 120-135.
36. Ust, Y. *Ecological performance analysis and optimization of power generation systems*. Diss. PhD thesis, Progress Report, Yildiz Technical University, Turkey, 2004 (in Turkish), 2004.
37. Ust, Yasin, Bahri Sahin, and Oguz Salim Sogut. "Performance analysis and optimization of an irreversible dual-cycle based on an ecological coefficient of performance criterion." *Applied energy* 82.1 (2005): 23-39.
38. Wijeysundera, N. E. "Simplified models for solar-powered absorption cooling systems." *Renewable energy* 16.1 (1999): 679-684.
39. Wouagfack, Paiguy Armand Ngouateu, and Réné Tchinda. "Performance optimization of three-heat-source irreversible refrigerators based on a new thermo-ecological criterion." *International Journal of Refrigeration* 34.4 (2011): 1008-1015.
40. Wouagfack, Paiguy Armand Ngouateu, and Réné Tchinda. "The new thermo-ecological performance optimization of an irreversible three-heat-source absorption heat pump." *International Journal of Refrigeration* 35.1 (2012): 79-87.
41. Wu, Chih, and Robert L. Kiang. "Finite-time thermodynamic analysis of a Carnot engine with internal irreversibility." *Energy* 17.12 (1992): 1173-1178.
42. Wu, Chin. "Cooling capacity optimization of a waste heat absorption refrigeration cycle." *Heat Recovery Systems and CHP* 13.2 (1993): 161-166.
43. Yan, Z. “Comment on Ecological optimization criterion for finite-time heat-engines”. *J. Appl. Phys. 73 (7), (1993): 35-83.*
44. Yan, Z. “Optimal performance of irreversible refrigerators.” *J. Refrig. (3), (1990)11-14.*
45. Yan, Z., and J. Chen. "An optimal endoreversible three-heat-source refrigerator." *Journal of Applied Physics* 65.1 (1989): 1-4.

46. Yilmaz, T. "A new performance criterion for heat engines: efficient power."*Journal of the Energy Institute* 79.1 (2006): 38-41.

47. Yilmaz, T. "Performance optimization of a Joule-Brayton engine based on the efficient power criterion." *Proceedings of the Institution of Mechanical Engineers, Part A: Journal of Power and Energy* 221.5 (2007): 603-607.

48. Ziegler, Felix. "State of the art in sorption heat pumping and cooling technologies." *International Journal of Refrigeration* 25.4 (2002): 450-459.